

---

# ATRAN3S: An Unsteady Transonic Code for Clean Wings

---

Guru P. Guruswamy, Peter M. Goorjian,  
and Fergus J. Merritt

---

FOR REFERENCE

FOR TO THE LIBRARY FROM THIS BOOK

December 1985

LIBRARY COPY

FEB 6 1986

LANGLEY RESEARCH CENTER  
LIBRARY, NASA  
HAMPTON, VIRGINIA



National Aeronautics and  
Space Administration



NF00046

---

# ATRAN3S: An Unsteady Transonic Code for Clean Wings

---

Guru P. Guruswamy, Informatics General Corporation, Palo Alto, California

Peter M. Goorjian, Ames Research Center, Moffett Field, California

Fergus J. Merritt, Informatics General Corporation, Palo Alto, California

December 1985



**Ames Research Center**  
Moffett Field, California 94035

186-31535

# ATRAN3S: AN UNSTEADY TRANSONIC CODE FOR CLEAN WINGS

Guru P. Guruswamy,\* Peter M. Goorjian, and Fergus J. Merritt†

Ames Research Center

## SUMMARY

This report explains the development and applications of the unsteady transonic code ATRAN3S for clean wings. Explanations of the unsteady, transonic small-disturbance aerodynamic equations that are used and their solution procedures are discussed. A detailed user's guide, along with input and output for a sample case, is given.

## INTRODUCTION

In the last decade, there have been extensive developments in computational unsteady transonic aerodynamics (ref. 1). Such developments are essential since the transonic regime plays an important role in the design of modern aircraft. For example, flight in the transonic regime provides the most efficient cruise performance because of the high lift-to-drag ratios that prevail under transonic conditions (ref. 2). However, it is at just such Mach numbers that the "dip" in the flutter curve (ref. 3) occurs. Consequently, there has been a large effort to develop computational tools with which to perform accurate flutter analyses at transonic speeds.

In the area of computational fluid dynamics (CFD), the unsteady, transonic aerodynamics are characterized by the feature of modeling the motion of shock waves over aerodynamic bodies, such as airfoils or wings. This modeling requires the solution of nonlinear partial differential equations. At the present time, the most advanced codes use the small-disturbance, transonic potential equation. These codes are being used for generic research in aeroelasticity. Currently, codes are being developed that use the more exact full-potential equation. In comparison, for steady flows, practical applications use full-potential codes, and there is extensive development of Euler codes.

The successful development of two-dimensional codes like LTRAN2 (ref. 4), which employ an alternating-direction-implicit (ADI), finite-difference scheme (ref. 1), and the availability of faster computers with more memory, make possible the

---

\*Principal Analyst, Informatics General Corporation, Palo Alto, California 94303.

†Program Analyst, Informatics General Corporation, Palo Alto, California 94303.

development and use of three-dimensional, unsteady transonic aerodynamic codes. An initial step was taken by Traci et al. (ref. 5) who developed the three-dimensional steady and unsteady small-disturbance codes TDSTRN and TDUTRN, respectively. The unsteady code TDUTRN is based on the harmonic method in which an unsteady solution is linearized with respect to time, and shock waves are fixed with respect to steady-state position. Thus, it is limited to the cases with very small oscillations. Eastep and Olsen (ref. 6) applied these codes to the computation of the flutter boundaries of a rectangular wing by using an uncoupled aeroelastic method.

Next, for more accuracy, Borland and Rizzetta (ref. 7) developed a three-dimensional, unsteady, small-disturbance transonic code, XTRAN3S, based on a time-integration method. In that code, the finite-difference scheme for two-dimensional flows employed in LTRAN2 (ref. 1) was extended to three-dimensional flows over wings. The unsteady equations of motion are time-accurately integrated by an ADI scheme that allows the shock waves to move. Also, this code can perform static and dynamic aeroelastic computations by simultaneously integrating the aerodynamic and structural equations of motion. The XTRAN3S code is being used for both aerodynamic and aeroelastic applications (refs. 8-10).

The use of XTRAN3S was limited to rectangular wings and wings with low sweep angle, large taper ratio, and large aspect ratio, such as transport aircraft wings. This limitation was due to the nature of the coordinate transformation that was used. The XTRAN3S code was not applicable to fighter-type wings, which are characterized by low aspect ratio, high sweep angle, and low taper ratio. Also, the code was not portable and it lacked some important features, a Fourier analyzing capability of the unsteady data. In order to overcome these limitations, a parallel improved code, ATRAN3S was developed at Ames Research Center. This code, which has a modified coordinate transformation along with many other new features, is applicable to both transport and fighter wings. This report explains the basic algorithm used in ATRAN3S, Version 1, and gives some typical examples.

#### FORMULATION OF UNSTEADY TRANSONIC-FLOW EQUATIONS

A discussion of the derivation of the three-dimensional, small-disturbance unsteady equations is given by Yoshihara (ref. 11). In accordance with reference 11, the modified small-disturbance equation for unsteady flow is written as

$$A\phi_{tt} + B\phi_{xt} = (E\phi_x + F\phi_x^2 + G\phi_y^2)_x + (\phi_y + H\phi_x\phi_y)_y + (\phi_z)_z \quad (1)$$

where  $A = M_\infty^2$ ;  $B = 2M_\infty^2$ ;  $E = (1 - M_\infty^2)$ ;  $F = -(1/2)(\gamma + 1)M_\infty^2$ ;  $G = -(1/2)(\gamma - 3)M_\infty^2$ ; and  $H = -(\gamma - 1)M_\infty^2$ . The coefficients F, G, and H are those proposed by Lomax et al. (ref. 12) when deriving the modified small-disturbance equation for steady flows.

The flow-field boundary conditions used are

$$\text{Far downstream: } \phi_x + k\phi_t = 0 \quad (2a)$$

$$\text{Far upstream: } \phi = 0 \quad (2b)$$

$$\text{Far above and below: } \phi_z = 0 \quad (2c)$$

$$\text{Far spanwise: } \phi_y = 0 \quad (2d)$$

$$\text{Wing root: } \phi_y = 0 \quad (2e)$$

$$\text{Trailing vortex wake: } [\phi_z] = 0 \quad (2f)$$

$$[\phi_x + k\phi_t] = 0 \quad (2g)$$

where the [ ] denotes the jump in the quantity across the vortex sheet.

The wing surface-flow tangency condition, which is satisfied at the mean chord plane, is given by

$$\phi_z = f_x + kf_t = 0 \quad (3)$$

where  $f_x$  denotes airfoil surface function; and where  $k = \omega c/U_\infty$  and is the reduced frequency based on the full root chord ( $\omega$  is the frequency in radians per second,  $c$  is a reference chord length, and  $U_\infty$  is the free-stream velocity).

#### Transformation for Swept-Tapered Wings

Equation (1), which is ideal for rectangular wings, can pose problems for swept tapered wings because of the dependence of its solution on leading-edge mesh spacing. Maintaining a sufficiently fine mesh spacing along the leading edge of a swept wing in a Cartesian coordinate system is inefficient because of the large number of points required. An alternative approach was developed by Ballhaus and Bailey (ref. 13). A shearing transformation was used to map a trapezoidal planform wing in the physical plane into a rectangle in the computational plane, as shown in figure 1 where

$$\xi(x, y) = (x - x_{LE})/c ; \quad \eta(y) = y ; \quad \zeta(z) = z \quad (4)$$

and where  $c$  is the local chord.

The leading and trailing edges lie on the coordinate lines  $\xi = 0$  and  $1$ , respectively. Use of this shearing transformation permits a more efficient distribution of mesh points, and each span station ( $\eta = \text{const}$ ) has the same number of chordwise mesh points on the wing surface. The problem of distributing grid points properly at the leading and trailing edges of the wing has been dealt with

precisely. This shearing transformation was used in XTRAN3S (ref. 7) throughout the flow field.

The conventional shearing transformation (4) is simple and adequate for wings with small sweep and large taper ratio. However, for wings with low aspect ratio, high sweep angle, and small taper ratio, such as fighter wings, this shearing transformation is not adequate. Since the transformation (4) is a function of local chord, the upstream and downstream far-field boundaries of the region in which the flow is computed depends on the planform. Thus, near those boundaries for delta-type wings (1) the coordinate lines are highly nonorthogonal, (2) the metrics have a large discontinuity in direction near the wing-tip span station, and (3) the flow is not normal to these boundaries. Thus, large discontinuities occur in the metric  $\xi_y$  along the tip span station. The metric appears as a coefficient for cross-derivatives. Also, in XTRAN3S the cross-derivatives have been differenced explicitly. These features of the shearing transformation can make the flow computations unstable, as has been illustrated for the F-5 wing (ref. 14).

In order to remove these disadvantages of the conventional shearing transformation, a modified shearing transformation was developed (ref. 14). The main requirement that any transformation should satisfy for the finite-difference method used in XTRAN3S is that it should map any given wing to a rectangular wing. This is satisfied in the modified shearing transformation by using the same conventional shearing transformation given by equation (4). However, for use away from the wing, a new scheme was devised such that the grid lines have the following properties: (1) far-field physical boundaries to the flow region are independent of the planform and always form the boundaries of a rectangular box, with the upstream and downstream surfaces normal to the free stream; (2) smaller gradients are obtained for the metric quantities, particularly near the boundaries, and smooth first and second derivatives are obtained for the metric quantities; and (3) grid lines are clustered near the leading and trailing edges as before for the shearing transformation. The details are given in reference 14.

After applying the transformation, equation (1) can be written as

$$-(A\xi_x^{-1}\phi_t + B\phi_\xi)_t + [E\xi_x^2\phi_\xi^2 + G(\xi_y\phi_\xi + \phi_\eta)^2 + \xi_x^{-1}\xi_y(\xi_y\phi_\xi + \phi_\eta) + H\xi_y\phi_\xi(\xi_y\phi_\xi + \phi_\eta)]_\xi + [\xi_x^{-1}(\xi_y\phi_\xi + \phi_\eta) + H\phi_\xi(\xi_y\phi_\xi + \phi_\eta)]_\eta + [\xi_x^{-1}\phi_\xi]_\zeta = 0 \quad (5)$$

The differencing procedure for equation (5) is an extension of the Murman-Cole type-dependent difference procedure applied to an arbitrary coordinate system (ref. 7). Type-dependent differences are used only to approximate derivatives in the streamwise direction, and all other derivatives are approximated by central differences. This method approximates the rotated differencing developed by Jameson (ref. 15). Thus the coefficient  $G$  is split into two components  $G_S$  and  $G_N$  where  $G_S = 1 - M_\infty^2$ , such that equation (5) may be decomposed into streamwise and normal contributions to the spatial differencing. Equation (5) can now be written as

$$-(A\xi_x^{-1}\phi_t + B\phi_\xi)_t + [E\xi_x\phi_\xi + F\xi_x^2\phi_\xi^2 + (G_S + G_N)(\xi_y\phi_\xi + \phi_\eta)^2 + \xi_x^{-1}\xi_y(\xi_y\phi_\xi + \phi_\eta) + H\xi_y\phi_\xi(\xi_y\phi_\xi + \phi_\eta)]_\xi + [\xi_x^{-1}(\xi_y\phi_\xi + \phi_\eta) + H\phi_\xi(\xi_y\phi_\xi + \phi_\eta)]_\eta + [\xi_x^{-1}\phi_\zeta]_\zeta = 0 \quad (6)$$

where

$$G = G_S + G_N ; \quad G_S = 1 - M_\infty^2 ; \quad G_N = (1/2)(\gamma - 2)M_\infty^2 - 1$$

Equation (6) is solved by a time-accurate ADI scheme. Details can be found in references 4 and 7.

### Viscous Corrections

Inviscid codes can provide reasonably good physical descriptions of the flow for cases in which viscous effects are not significant. Viscous effects, when significant, can cause (1) an altering of shock strength and location because of shock and boundary-layer interaction; (2) camber modifications because of differences in the boundary-layer displacement on the upper and lower airfoil surfaces; and (3) displacement and camber effects near the wake. These viscous effects in turn may influence aeroelastic characteristics. These effects can be accounted for by linking the inviscid calculations with boundary-layer corrections. Two viscous models, the viscous ramp and the Green lag-entrainment models were considered. Both the ramp model and the lag-entrainment equations, which were derived for steady-state computations, are incorporated in a quasi-steady fashion for unsteady computations. Thus, these viscous models may lose accuracy at higher frequencies.

Viscous computing capabilities were incorporated in the Boeing version of XTRAN3S by Rizzetta and Borland (ref. 16). By exercising that code, we noticed that the lift and moment results displayed high-frequency oscillations. This numerical instability was traced back to the incompatibilities in the procedure for computing the shock locations which are required to apply viscous corrections. Incompatibilities occurred because the three-dimensional shock profile was used to model the two-dimensional viscous corrections. In ATRAN3S, this instability was corrected by using a two-dimensional shock profile to model the two-dimensional viscous corrections. That correction eliminated the source of numerical instability in implementing the viscous wedge model in three-dimensional computations. With this modified viscous correction method, several computations were made for a rectangular and a transport-type wing; they are discussed in reference 17.

### Aeroelastic Computations

ATRAN3S can be used for both coupled (ref. 18) and uncoupled (ref. 8) aeroelastic computations. The simultaneous integration procedure developed for airfoils (refs. 19 and 20) has been extended to wings, and it is incorporated in the code.

## INPUT

The detailed input for the code is given in appendix A. Some important portions of the input are described in this section. The type of input used in XTRAN3S is not portable from computer to computer. In ATRAN3S, the input is in the form of NAMELIST, which is available on main frame computers such as the Cray, CYBER, and VAX.

### Grid

After transformation, the flow equations are solved in a Cartesian coordinate system. In any finite-difference scheme the grid plays an important role in obtaining the solution. The correct number of grid points and their proper distribution are essential. For the default grid system in the code, the grid is designed to obtain the best possible solution. The grid system has 64 points in the streamwise direction, 40 in the vertical direction, and 20 in the spanwise direction. The wing surface was defined by 39 points in the streamwise direction and 13 points in the spanwise direction. Computational boundaries are located as follows: the upstream boundary was at 15.4 chords; the downstream boundary was at 26.6 chords; the far-span boundary was at 1.6 semispan; and the far-field boundary was at 25.0 chords above the wing and at 25.0 chords below the wing. Grid points were generated such that the first and second derivatives of the grid lines were smooth. Plots of this grid in the  $\xi$ - $\eta$  plane and  $\xi$ - $\zeta$  plane are shown in figures 2 and 3, respectively. In figure 3, the grid is smoothly stretched in an exponential manner in the  $\zeta$ -direction away from the plane of the wing ( $\zeta = 0$ ). This smooth stretching removes a deficiency of the original XTRAN3S grid in the  $\zeta$ -direction. In figure 2 it can be seen that in the interest of accuracy the grid is clustered near the leading and trailing edges in the  $\xi$ -direction. Also, grid boundaries are located far away from the wing to avoid boundary reflections. And again for accuracy, the grid spacing in the  $\eta$ -direction is fine near the tip.

### Convergence and Time-Step Size

Steady aerodynamic pressures are computed by integrating equation (5) in time and setting steady boundary conditions on the wing. ATRAN3S does not compute the residuals of the velocity potential to determine the convergence to a steady-state solution. Convergence can be determined by examining the pressure coefficient. The integration procedure may be stopped when the maximum pressure coefficient on the wing does not change by more than about 0.1% over 100 time-steps. This has given results that compare fairly well with experiment. The number of time-steps and the time-step size required for convergence depend mainly on the planform and the Mach number.

Unsteady aerodynamic forces are computed by having the wing undergo a given motion and then integrating the aerodynamic equation of motion in time. The code

has the capability of accounting for sinusoidal motion of rigid wings and for modal motions of flexible wings. In the many cases studied, it was found that about three cycles of motion are sufficient to obtain a periodic aerodynamic response. Periodicity was tested by comparing the Fourier coefficients of the responses between the second and third cycles. This feature of generating the Fourier coefficients as part of the ATRAN3S output data is an improvement over the original version of XTRAN3S.

## ILLUSTRATION

### Swept Tapered Wing

The original version of XTRAN3S was not adequate for fighter-type wings which are characterized by low aspect ratio, high sweep angle, and small taper ratio. For example, as shown in figure 4, the planform of the F-5 wing has an aspect ratio of 3.0, a taper ratio of 0.3, and a leading-edge sweep of  $32^\circ$ . Preliminary attempts made by using the earlier version of XTRAN3S (ref. 7) to obtain steady and unsteady results for this wing were not successful. The code was unstable even at the very small time-step size of 0.001, which is too small for routine use. At this time-step size, unsteady computations would require about 30,000 time-steps per cycle at a reduced frequency of 0.2. This failure was due to the conventional shearing transformation used in the original version of XTRAN3S. In the improved version, ATRAN3S, the problem was eliminated by using the modified shearing transformation (ref. 14).

Figure 5 shows the physical grid obtained from the conventional shearing transformation which made the flow computations unstable. The physical grid obtained by the modified transformation (ref. 14) is shown in figure 6, which has made the flow computations more stable and accurate. Figure 7 shows the plots of steady-pressure results obtained at  $M = 0.9$  for the 50% semispan station. In spite of using a time-step size of 0.001, results from the conventional shearing transformation diverged before reaching 6,000 time-steps. Also, the results were highly inaccurate before diverging, as shown at 4,000 time-steps in figure 7. A converged solution was obtained by using 2,000 time-steps of size 0.01 with the modified shearing transformation. It can be seen that the latter method compares well with experiment (ref. 21). Plots of steady pressure distributions obtained by the modified transformation and experiment are given for four span stations in figure 8. Comparisons are good at all span stations.

Figure 9 shows the modal motion used in the NLR experiment (ref. 21) where the F-5 wing is pitching about an axis normal to the root chord and located at 50% of root chord. Figure 10 shows the plots of real and imaginary values of upper-surface pressures at four span stations obtained by the modified shearing transformation and the NLR experiment at  $M = 0.9$  at a frequency of 40 Hz. The same modal motion used in the experiment was simulated in the code. Results from the code were obtained by oscillating the wing in a sinusoidal modal motion for three cycles, with

1,200 time-steps per cycle during which transients disappeared and a periodic response was obtained. Results from the code compare well with the experimental measurements (ref. 21). It is noted here that no attempt was made to use the conventional shearing transformation because of the diverged results in the steady calculations.

The input and output data for this case are given in appendix B.

#### SALIENT PROGRAMMING FEATURES OF ATRAN3S

The complete ATRAN3S program is written in FORTRAN without any machine-dependent statements. The input and output processors in the original version depend on the computer, whereas in the Ames version they are independent of computers. The standard NAMELIST-type of input is used. The input can be very easily interfaced with any data-generation packages at the user end. The input can accept either coordinates or slopes of the wing surface instead of the polynomial representation required by the original version. Many options are provided in the output processor. The present output processor uses about 15% less computer time than that in XTRAN3S. Also it has some special features such as a Fourier analysis package for unsteady results. Finally, the ATRAN3S can handle both fighter- and transport-type wings.

At present the code is being exercised on a Cray X-MP. The memory required for a  $64 \times 40 \times 20$  grid is about 500K words. The code is operating at a speed of 8.92  $\mu$ sec per grid point per operation on the Cray X-MP with a single processor. The code is easily portable to other computers.

APPENDIX A  
DESCRIPTION OF ATRAN3S INPUT

FIRST CARD Title written in 'A' FORMAT (Maximum 60 characters)  
 The rest of the INPUT is in NAMELIST format in the order described below

NAMELIST	VARIABLE	TYPE	DEFAULT	DESCRIPTION
1 NREST				Restart condition data
	a) RESTRT	LOGI	FALSE	Flag to specify restart TRUE - restart FALSE - no restart
2 NPRNT				Flags to control output
	a) IPRFLG1	INT	0	Flag for special debug output 0 - normal output 1 - debug output
	b) IPRFREP	INT	1	Pressure data print frequency (in time steps)
	c) IPRFREF	INT	1	Force data print frequency
	d) IPRFRED	INT	1	Displacement data print frequency
	e) IPLFRED	INT	1	Displacement plot data frequency
	f) SKIPCYC	INT	0	Pressure data print frequency (in cycles)
3 NTASK				Task type data
	a) TASK	HOLL	'TASK3'	Control to specify type of task (static or dynamic) 'TASK2' - for static cases 'TASK3' - for dynamic case
	b) AEROTSK	HOLL	' '	Flag indicating aeroelastic solution 'FLEXIBLE' - solution is aero- elastic ' ' - solution not aero- elastic
4 NFLWP				Flow Parameters
	a) MACHNO	REAL	0 8	Mach Number
	b) UFS	REAL	1 0	Velocity
	c) GAMMA	REAL	1 4	Ratio of specific heats
	d) REDFREQ	REAL	1 0	Reduced frequency
5 NITER				Computational Parameters
	a) ITER	INT	0	Number of time steps completed (RESTART)
	b) MAXITS	INT	0	Maximum steady iterations
	c) MAXITD	INT	1000	Maximum unsteady iterations
	d) T	REAL	0 0	Time elapsed (RESTART)
	c) DELTAT	REAL	0 1745329	Time step size
6 NEQUA				Equation Parameters

a) EQ HOLL 'MODI' Type of small disturbance equation  
 'MODI' - modified  
 'CLAS' - classical  
 b) MODIFY HOLL 'AMES' Type of coefficients in modified  
 'AMES' - Ames coefficients  
 'NLR' - NLR coefficients  
 c) FREQ HOLL 'HIGH' Type of frequency approximation  
 'HIGH' - high frequency  
 'LOW' - low frequency

8 NMSET Y - Grid Lines (eta)

a) NETAT	INT	20	Total number of grid lines
b) NETAIB	INT	13	Number of grid lines inboard of tip (inclusive)
c) NETAOB	INT	7	Number of grid lines outboard of tip (exclusive)
d) ETA	REAL	(Apndx A-1)	NETAT values of grid lines

9 NMSHZ Z - Grid Lines (zeta)  
 a) NZT INT 40 Total number of grid lines  
 b) NZU INT 20 Grid lines above wing  
 c) NZL INT 20 Grid lines below wing  
 d) ZETA REAL (Apndx A-1) NZT values of grid lines

10 NWPLN Planform data  
a) FORMAT HOLL 'RATIO' Format of planform input  
'RATIO' - planform is described as ratios

Note If FORMAT='RATIO' then following INPUT is required

b) ARATIO REAL 4.0 Aspect ratio  
 c) TRATIO REAL 1.0 Taper ratio  
 d) SWANGL REAL 0.0 Mean angle of attack in degrees  
 e) NAIRSEC INT 2 Number of sections at which airfoil sections are defined  
 f) SLPINP LOGI FALSE Flag to control type of airfoil section input  
 TRUE - sections are described by slopes  
 FALSE - sections are described by coordinates

## 11 NAIR

Definition of airfoil section. This  
NAMELIST data is repeated NAIRSEC  
times (see NAMELIST NWPLN)

a) YVAL	REAL	0.0	Eta value of span station
b) NINU	INT	48	Number of points on upper surface
c) NINL	INT	48	Number of points on lower surface
d) XINU	REAL	(Apndx A-2)	X-Coordinates for upper surface
e) XINL	REAL	(Apndx A-2)	X-Coordinates for lower surface
f) ZINU	REAL	(Apndx A-2)	Z-Coordinates or slopes for upper surface
g) ZINL	REAL	(Apndx A-2)	Z-Coordinates or slopes for lower surface

## 12 NDYN

## Boundary condition data

a) MOTYPE	HOLL	'MODA'	Flag indicating motion type 'SINU' - sinusoidal 'MODA' - modal
b) SUBCASE	HOLL	', '	Flag indicating dynamic subcase to be executed when MOTYPE = 'SINU' 'PITC' - pitch 'PLUN' - plunge

The following data groups depend on value of MOTYPE

## Data for indicial motion (MOTYPE = 'INDI')

Ic) ALPHIM	REAL	0 1	Amplitude of indicial plunge effective angle (in degrees)
Id) QSUBIM	REAL	0 1	Amplitude of indicial pitch (in degrees/second)
Ie) XROTIM	REAL	0 5	X coordinate of axis rotation (fraction of reference chord)

## Data for sinusoidal motion (MOTYPE = 4LSINU)

When SUBCASE = 4LPLUN

Sc) OMEGSR	REAL	0 2	Frequency of plunging motion (in radians/sec )
Sd) H1SM	REAL	0 1	Amplitude of plunging motion (fraction of reference chord)
Se) PHESP	REAL	0 0	Phase of plunging motion (in radians)

When SUBCASE = 4LPITC

Sf) OMEGSP	REAL	0 2	Frequency of pitching motion (in radians/sec )
Sg) ALPHSM	REAL	1 0	Amplitude of pitching motion (in degrees)
Sh) XROTSM	REAL	0 5	X-coordinate of axis of pitching (fraction of reference chord)
Si) PHESR	REAL	0 0	Phase for sinusoidal motion (in radians)

## Data for modal motion (MOTYPE = 4LMODA)

Mc) NMODES	INT	1	Number of modes in case (maximum = 20)
Md) MODENO	INT	1	Index of current mode
Me) FREQMD	REAL	0 1	Frequency of oscillation for sinusoidal motion of current mode (in radians)
Mf) AMPMD	REAL	1 0	Amplitude of displacement for current mode
Mg) PHASEMD	REAL	0 0	Phase of oscillation for current mode

Note The following NAMELIST data should be present only if the motion type is modal (MOTYPE = 4LMDA). This data group is repeated NXIW (NXIT-NXIF-NXIA) times (see NAMELIST NMSXI)

13 NMODE	Numerical description of slopes and displacements		
a) MODEN	INTE	0	Mode sequence number
b) ISPLAN	INTE	0	Span station sequence number
c) DDISP	REAL	NONE	Mode displacements mapped to XI grid on the wing

Note The NAMELIST data entry features vector array filling, therefore it is not necessary to include zero values at the end of each vector array

14 NBUND	Boundary condition flags		
a) BCSYMM	HOLL	'Y'	Flag specifying configuration symmetry 'Y' - Y=0 is plane of symmetry 'Z' - Z=0 is plane of symmetry 'BOTH' - Y=0 and Z=0 are both planes of symmetry 'NONE' - Configuration has no symmetry
b) DOWNST	HOLL	'UNST'	Flag specifying downstream boundary condition 'STEA' - Downstream boundary con- dition is steady 'UNST' - Downstream boundary con- dition is unsteady
c) FARFLD	HOLL	'FREE'	Flag specifying farfield boundary condition 'FREE' - Farfield B C is freejet 'AIRF' - Farfield B C is airfoil 'KLUN' - Farfield B C is klunker
d) LOWER	HOLL	'ZERO'	Flag specifying lower farfield boundary condition 'ZERO' - Velocity at lower boundary is zero 'CALC' - Velocity at lower boundary is calculated
e) UPPER	HOLL	'ZERO'	Flag specifying upper farfield boundary condition 'ZERO' - Velocity at upper boundary is zero 'CALC' - Velocity at upper boundary is calculated

f)	UPSTRM	HOLL	'FREE'	Flag specifying upstream boundary condition 'FREE' - Boundary condition is freestream (only choice)
g)	WAKEBC	HOLL	'UNST'	Flag specifying jump condition to be applied to potential across the wake 'STEA' - Steady jump condition to be applied 'UNST' - Unsteady jump condition to be applied
h)	WALLS	HOLL	'NONE'	Flag specifying wind tunnel wall boundary condition to be applied 'UPPE' - Walls are to be used for upper and lower boundaries 'SIDE' - Walls are to be used for side boundaries 'BOTH' - Walls are to be used for upper, lower and side boundaries 'NONE' - Walls are not used as boundaries
i)	WINGBC	HOLL	'UNST'	Flag specifying lifting surface boundary condition 'STEA' - Lifting surface B C is steady 'UNST' - Lifting surface B C is unsteady

#### 15 NANGL

Angles of attack

a)	ALPHREF	REAL	0 0	Rigid angle of attack
----	---------	------	-----	-----------------------

#### 16 NREFV

Geometry reference data

a)	SREF	REAL	4 0	Reference area
b)	CBAR	REAL	1 0	Mean aerodynamic chord
c)	XMOMC	REAL	0 5	Moment center reference
d)	CREF	REAL	1 0	Reference chord
e)	BREF	REAL	3 0	Reference span
f)	XZERO	REAL	0 5	Moment reference variable

Note The following four NAMELIST data should be present only if the solution is aeroelastic (AEROTSK = 'FLEXIBLE') NMODE is repeated NMAES \* NETAIB times (see NAMELISTS NARO1 and NMSET) NARO3 is repeated NMAES times (see NAMELIST NARO1)

#### 17 NARO1

Aeroelastic solution control data  
Required only if AEROTSK='FLEXIBLE'

a)	NMAES	INT	5	Number of generalized coordinates for the aeroelastic solution (maximum = 20)
b)	NEFAES	INT	20	Number of points which have external forces defined in the aeroelastic solution (maximum = 20)
c)	NSAES	INT	50	Number of structural degrees of freedom (maximum = 50)
d)	NSUBZAE	REAL	1 0	Structural load factor
e)	GRAVAE	REAL	1 0	Acceleration due to gravity

f) QAE	REAL	1 0	Dynamic pressure
g) CSUBR	REAL	1 0	Reference chord for aeroelastic solution
18 NMODE		Aeroelastic modal displacements Required only if AEROTSK='FLEXIBLE'	
a) MODEN	INTE	0	Mode sequence number
b) ISPLAN	INTE	0	Span station sequence number
c) DDISP	REAL	NONE	Mode displacements mapped to XI grid on the wing
19 NAR02		Structural matrix data Required only if AEROTSK='FLEXIBLE'	
a) DMAE	REAL	no default	Generalized mass matrix
b) DDAE	REAL	no default	Generalized damping matrix
c) DKAE	REAL	no default	Generalized stiffness matrix
Note It is not necessary to include zero values at the end of each vector array			
20 NAR03		Initial conditions generalised displacements Required only if AEROTSK='FLEXIBLE'	
a) GENP1	REAL	0 0	Generalised displacements
b) DGENP1	REAL	0 0	Generalised velocities
c) DDGENP1	REAL	0 0	Generalised accelerations
21 NVIS		Boundary layer correction	
a) VISC	LOGI	FALSE	Viscous calculation indicator TRUE - Yes FALSE - No
b) GREEN	LOGI	FALSE	Boundary layer indicator TRUE - Yes FALSE - No
c) WEDGE	LOGI	FALSE	Wedge calculation indicator TRUE - Yes FALSE - No
d) READV	LOGI	FALSE	Viscous restart indicator TRUE - On FALSE - Off
e) IBLCN	INT	0	Boundary layer calculation counter
f) IBLPN	INT	0	Boundary layer print counter
g) IBLCAL	INT	1	Boundary layer calculation interval
h) IBLPRT	INT	50	Boundary layer print interval
i) XOFFST	REAL	0 02	Ramp shock offset length
j) XPREC	REAL	0 02	Ramp precursor length
k) XRAMP	REAL	0 10	Ramp length

#### APPENDIX A-1 DEFAULT GRID VALUES

XI VALUES		ETA VALUES		ZETA VALUES	
I	XI	I	XI	J	Y
				K	Z

1	-15	3750	33	0.4600	1	-0	2000	1	-24	9140
2	-8	1079	34	0.4900	2	0	0000	2	-13	6750
3	-4	2473	35	0.5200	3	0	2000	3	-7	7280
4	-2	2050	36	0.5500	4	0	4000	4	-4	5020
5	-1	1318	37	0.5800	5	0	6000	5	-2	7060
6	-0	5737	38	0.6100	6	0	8000	6	-1	6800
7	-0	2881	39	0.6400	7	0	9999	7	-1	0780
8	-0	1453	40	0.6700	8	1	1989	8	-0	7140
9	-0	0758	41	0.7000	9	1	3931	9	-0	4880
10	-0	0426	42	0.7300	10	1	5736	10	-0	3440
11	-0	0259	43	0.7600	11	1	7289	11	-0	2480
12	-0	0151	44	0.7900	12	1	8536	12	-0	1840
13	-0	0050	45	0.8199	13	1	9535	13	-0	1380
14	0	0050	46	0.8497	14	2	0419	14	-0	1050
15	0	0151	47	0.8788	15	2	1357	15	-0	0800
16	0	0254	48	0.9066	16	2	2605	16	-0	0610
17	0	0365	49	0.9326	17	2	4632	17	-0	0450
18	0	0494	50	0.9566	18	2	8085	18	-0	0320
19	0	0649	51	0.9788	19	3	3363	19	-0	0200
20	0	0839	52	1.0000	20	4	0000	20	-0	0100
21	0	1065	53	1.0219				21	0	0100
22	0	1324	54	1.0516				22	0	0200
23	0	1607	55	1.1037				23	0	0320
24	0	1901	56	1.2036				24	0	0450
25	0	2200	57	1.3947				25	0	0610
26	0	2500	58	1.7521				26	0	0800
27	0	2800	59	2.4048				27	0	1050
28	0	3100	60	3.5750				28	0	1380
29	0	3400	61	5.6456				29	0	1840
30	0	3700	62	9.2758				30	0	2480
31	0	4000	63	15.6006				31	0	3440
32	0	4300	64	26.5750				32	0	4880
								33	0	7140
								34	1	0780
								35	1	6800
								36	2	7060
								37	4	5020
								38	7	7280
								39	13	6750
								40	24	9140

## APPENDIX B

ATRAN3S INPUT/OUTPUT FOR F-5 WING UNDERGOING MODAL OSCILLATIONS

THE F-5 WING UNDERGOING MODAL OSCILLATIONS AT M=0 9 AND K = 0 55(40HZ)

\$NREST RESTRT= FALSE \$  
 \$NPRNT IPRFLG1=0,IPRFREP=1000,IPRFREF=1000,IPRFRED=1,IPLFRED=1,SKIPCYC=0 \$  
 \$NTASK TASK='TASK3' \$  
 \$NFLWP MACHNO = 0 90,GAMMA=1 4\$  
 \$NITER MAXITS=0,MAXITD=3500,ITER=0,T=0 0,DELTAT = 0.01 \$  
 \$NEQUA FREQ=4LHIGH \$  
 \$NMSXI  
 NXIT=64,NXIF=13,NXIA=12,  
 XI= -15 37500,-8 10791,-4 24734,-2 20500,-1 13177,  
 -0 57371,-0 28812,-0 14526,-0 07579,-0 04260,  
 -0 02589,-0 01506,-0 00500  
 0 00500,0 01506,0 02539,0 03653,0 04938,  
 0 06493,0 08391,0 10654,0 13245,0 16067,  
 0 19012,0 22001,0 25000,0 28000,0 31000,  
 0 34000,0 37000,0 40000,0 43000,0 46000,  
 0 49000,0 52000,0 55000 0 58000,0 61000,  
 0 64000,0 67000,0 70000,0 73000,0 76000,  
 0 79000,0 81994,0 84966,0 87875,0 90659,  
 0 93262,0 95660,0 97881,  
 1 00000,1 02188,1 05155,1 10369,1 20357,  
 1 39472,1 75209,2 40476,3 57502,5 64564,  
 9 27579,15 60064,26 57500\$  
 \$NMSET NETAOB= 7,NETAIB=13,  
 ETA= -0 0973,0 0000,0 0973,0 1947,0 2920,0 3894,0 4867,  
 0 5835,0 6780,0 7659,0 8415,0 9022,0 9508,  
 0 9938,1 0394,1 1002,1 1988,1 3669,1 6238,1 9468 \$  
 \$NMSH7 ZETA= -24 914, -13 675, -7 728, -4 502, -2 706, -1 680, -1 078, -0 714,  
 -0 488, -0 344, -0 248, -0 184, -0 138, -0 105, -0 080, -0 061, -0 045, -0 032, +0 020,  
 -0 010,0 010,0 020,0 032,0 045,0 061,0 080,0 105,0 138,0 184,0 248  
 0 344,0 488,0 714,1 078,1 680,2 706,4 502,7 728,13 675,24 914 \$  
 \$NWPLN FORMAT='RATIO',ARATIO = 2 9768,TRATIO=0 308,SWANGL=31 917,NATRSEC=2,  
 SLPINP= TRUE \$  
 \$NAIR YVAL=0 00, NINU=39, NINL=39,  
 XINU=0 005,0 015,0 025,0 035,0 045,0 060,0 080,0 100,0 130,  
 0 160,0 190,0 220,0 250,0 280,0 310,0 340,0 370,0 400,  
 0 430,0 460,0 490,0 520,0 550,0 580,0 610,0 640,0 670,  
 0 700,0 730,0 760,0 790,0 820,0 850,0 880,0 910,0 935,  
 0 960,0 980,1 000,  
 XINL=0 005,0 015,0 025,0 035,0 045,0 060,0 080,0 100,0 130,  
 0 160,0 190,0 220,0 250,0 280,0 310,0 340,0 370,0 400  
 0 430,0 460,0 490,0 520,0 550,0 580,0 610,0 640,0 670,  
 0 700,0 730,0 760,0 790,0 820,0 850,0 880,0 910,0 935,  
 0 960,0 980,1 000,  
 ZINU=0 31365,0 23291,0 20255,0 18295,0 16790,  
 0 14974,0 13017,0 11384,0 09336,0 07637,  
 0 06202,0 04978,0 03925,0 03012,0 02214,  
 0 01508,0 00875,0 00300,-0 00233,-0 00733,  
 -0 01212,-0 01676,-0 02130,-0 02580,-0 03026,  
 -0 03469,-0 03905,-0 04333,-0 04745,-0 05134,  
 -0 05492,-0 05806,-0 06065,-0 06252,-0 06352,  
 -0 06356,-0 06274,-0 06139,-0 05935,  
 ZINL=-0 27687,-0 11999,-0 07540,-0 05394,-0 04169  
 -0 03137,-0 02474,-0 02184,-0 02041,-0 02020  
 -0 02009,-0 01960,-0 01852,-0 01677,-0 01438,  
 -0 01137,-0 00780,-0 00377,0 00065,0 00537  
 0 01030,0 01537,0 02049,0 02558,0 03056,

```

0 03538,0 03997,0 04427,0 04823,0 05181,
0 05496,0 05765,0 05986,0 06157,0 06275
0 06334,0 06356,0 06348,0 06316$  

$NAIR YVAL=0 9734,NINU=39,NINL=39,
XINU=0 005,0 015,0 025,0 035,0 045,0 060,0 080,0 100,0 130,
0 160,0 190,0 220,0 250,0 280,0 310,0 340,0 370,0 400,
0 430,0 460,0 490,0 520,0 550,0 580,0 610,0 640,0 670,
0 700,0 730,0 760,0 790,0 820,0 850,0 880,0 910,0 935,
0 960,0 980,1 000,
XINL=0 005,0 015,0 025,0 035,0 045,0 060,0 080,0 100,0 130,
0 160,0 190,0 220,0 250,0 280,0 310,0 340,0 370,0 400,
0 430,0 460,0 490,0 520,0 550,0 580,0 610,0 640,0 670,
0 700,0 730,0 760,0 790,0 820,0 850,0 880,0 910,0 935,
0 960,0 980,1 000,
ZINU=0 31365,0 23291,0 20255,0 18295,0 16790,
0 14974,0 13017,0 11384,0 09336,0 07637,
0 06202,0 04978,0 03925,0 03012,0 02214,
0 01508,0 00875,0 00300,-0 00233,-0 00733,
-0 01212,-0 01676,-0 02130,-0 02580,-0 03026,
-0 03469,-0 03905,-0 04333,-0 04745,-0 05134,
-0 05492,-0 05806,-0 06065,-0 06252,-0 06352,
-0 06356,-0 06274,-0 06139,-0 05935,
ZINL=-0 27687,-0 11999,-0 07540,-0 05394,-0 04169,
-0 03137,-0 02474,-0 02184,-0 02041,-0 02020,
-0 02009,-0 01960,-0 01852,-0 01677,-0 01438,
-0 01137,-0 00780,-0 00377,0 00065,0 00537,
0 01030,0 01537,0 02049,0 02558,0 03056,
0 03538,0 03997,0 04427,0 04823,0 05181,
0 05496,0 05765,0 05986,0 06157,0 06275,
0 06334,0 06356,0 06348,0 06316$  

$NDYN MOTYPE=4LMODA,FREQMD=0 550,AMPMD=1 0,PHASEMD=0 0 $  

$NMODE DD1SP =
-0 00652, -0 00650, -0 00650, -0 00649, -0 00646,
-0 00641, -0 00632, -0 00618, -0 00599, -0 00575,
-0 00546, -0 00515, -0 00346, -0 00308, -0 00271,
-0 00233, -0 00196, -0 00158, -0 00121, -0 00083,
-0 00046, -0 00010, 0 00026, 0 00060, 0 00095,
0 00128, 0 00161, 0 00193, 0 00225, 0 00257,
0 00291, 0 00327, 0 00404, 0 00440, 0 00475,
0 00508, 0 00538, 0 00565, 0 00592,
DSLOP =
0 01184, 0 01184, 0 01184, 0 01184, 0 01184,
0 01184, 0 01184, 0 01184, 0 01184, 0 01184,
0 01184, 0 01184, 0 01184, 0 01184, 0 01184,
0 01184, 0 01184, 0 01184, 0 01184, 0 01184,
0 01184, 0 01184, 0 01184, 0 01184, 0 01184,
0 01184, 0 01184, 0 01184, 0 01184, 0 01184,
$  

$NMODE DDISP =
-0 00652, -0 00650, -0 00650, -0 00649, -0 00646,
-0 00641, -0 00632, -0 00618, -0 00599, -0 00575,
-0 00546, -0 00515, -0 00346, -0 00308, -0 00271,
-0 00233, -0 00196, -0 00158, -0 00121, -0 00083,
-0 00046, -0 00010, 0 00026, 0 00060, 0 00095,
0 00128, 0 00161, 0 00193, 0 00225, 0 00257,
0 00291, 0 00327, 0 00404, 0 00440, 0 00475,
0 00508, 0 00538, 0 00565, 0 00592,
DSLOP =
0 01184, 0 01184, 0 01184, 0 01184, 0 01184.

```

```

0 01184, 0 01184, 0 01184, 0 01184, 0 01184.
0 01184, 0 01184, 0 01184, 0 01184, 0 01184.
0 01184, 0 01184, 0 01184, 0 01184, 0 01184.
0 01184, 0 01184, 0 01184, 0 01184, 0 01184.
0 01184, 0 01184, 0 01184, 0 01184, 0 01184.
0 01184, 0 01184, 0 01184, 0 01184, 0 01184.
0 01184, 0 01184, 0 01184, 0 01184, 0 01184.
$  

$NMODE DDISP =
-0 00576, -0 00575, -0 00574, -0 00573, -0 00571,
-0 00566, -0 00558, -0 00545, -0 00528 -0 00506
-0 00480, -0 00451, -0 00291, -0 00257, -0 00222.
-0 00187, -0 00152, -0 00117, -0 00082, -0 00047.
-0 00012, 0 00021, 0 00055, 0 00087, 0 00119.
0 00150, 0 00180, 0 00209, 0 00239, 0 00268.
0 00300, 0 00332, 0 00406, 0 00440, 0 00472.
0 00503, 0 00531, 0 00556, 0 00581,
DSLOP =
0 01184, 0 01184, 0 01184, 0 01184, 0 01184,
0 01184, 0 01184, 0 01184, 0 01184, 0 01184.
0 01184, 0 01184, 0 01184, 0 01184, 0 01184.
0 01184, 0 01184, 0 01184, 0 01184, 0 01184.
0 01184, 0 01184, 0 01184, 0 01184, 0 01184.
0 01184, 0 01184, 0 01184, 0 01184, 0 01184.
0 01184, 0 01184, 0 01184, 0 01184, 0 01184.
$  

$NMODE DDISP =
-0 00501, -0 00499, -0 00498, -0 00497, -0 00495,
-0 00491, -0 00484, -0 00473, -0 00458, -0 00438.
-0 00414, -0 00388, -0 00237, -0 00205, -0 00173.
-0 00140, -0 00108, -0 00076, -0 00043, -0 00011.
0 00021, 0 00053, 0 00084, 0 00114, 0 00143.
0 00172, 0 00199, 0 00226, 0 00253, 0 00280.
0 00308, 0 00337, 0 00409, 0 00440, 0 00470.
0 00498, 0 00524, 0 00548, 0 00570,
DSLOP =
0 01184, 0 01184, 0 01184, 0 01184, 0 01184,
0 01184, 0 01184, 0 01184, 0 01184, 0 01184.
0 01184, 0 01184, 0 01184, 0 01184, 0 01184.
0 01184, 0 01184, 0 01184, 0 01184, 0 01184.
0 01184, 0 01184, 0 01184, 0 01184, 0 01184.
0 01184, 0 01184, 0 01184, 0 01184, 0 01184.
0 01184, 0 01184, 0 01184, 0 01184, 0 01184.
$  

$NMODE DDISP =
-0 00426, -0 00424, -0 00422, -0 00421, -0 00420.
-0 00416, -0 00410, -0 00400, -0 00387, -0 00369.
-0 00348, -0 00324, -0 00183, -0 00153, -0 00124.
-0 00094, -0 00064, -0 00035, -0 00005, 0 00025.
0 00055, 0 00084, 0 00113, 0 00141, 0 00167.
0 00193, 0 00218, 0 00243, 0 00266, 0 00291.
0 00316, 0 00343, 0 00411, 0 00440, 0 00467.
0 00493, 0 00517, 0 00539, 0 00560,
DSLOP =
0 01184, 0 01184, 0 01184, 0 01184, 0 01184,
0 01184, 0 01184, 0 01184, 0 01184, 0 01184.
0 01184, 0 01184, 0 01184, 0 01184, 0 01184.
0 01184, 0 01184, 0 01184, 0 01184, 0 01184.
0 01184, 0 01184, 0 01184, 0 01184, 0 01184.

```



```

$NMODE DDISP =
-0 00127, -0 00124, -0 00122, -0 00121, -0 00120,
-0 00119, -0 00116, -0 00112, -0 00106, -0 00098,
-0 00086, -0 00073, 0 00032, 0 00051, 0 00070,
0 00090, 0 00109, 0 00129, 0 00148, 0 00168,
0 00187, 0 00208, 0 00228, 0 00246, 0 00264,
0 00280, 0 00295, 0 00308, 0 00321, 0 00335,
0 00349, 0 00364, 0 00420, 0 00439, 0 00457,
0 00474, 0 00489, 0 00503, 0 00517,
DSLOP =
0 01184, 0 01184, 0 01184, 0 01184, 0 01184,
0 01184, 0 01184, 0 01184, 0 01184, 0 01184,
0 01184, 0 01184, 0 01184, 0 01184, 0 01184,
0 01184, 0 01184, 0 01184, 0 01184, 0 01184,
0 01184, 0 01184, 0 01184, 0 01184, 0 01184,
0 01184, 0 01184, 0 01184, 0 01184, 0 01184,
0 01184, 0 01184, 0 01184, 0 01184, 0 01184,
$ 
$NMODE DDISP =
-0 00059, -0 00056, -0 00054, -0 00053, -0 00052,
-0 00051, -0 00050, -0 00047, -0 00042, -0 00036,
-0 00027, -0 00016, 0 00080, 0 00098, 0 00115,
0 00132, 0 00149, 0 00166, 0 00183, 0 00200,
0 00217, 0 00236, 0 00254, 0 00270, 0 00286,
0 00299, 0 00312, 0 00323, 0 00334, 0 00345,
0 00356, 0 00369, 0 00422, 0 00438, 0 00454,
0 00469, 0 00483, 0 00495, 0 00507,
DSLOP =
0 01184, 0 01184, 0 01184, 0 01184, 0 01184,
0 01184, 0 01184, 0 01184, 0 01184, 0 01184,
0 01184, 0 01184, 0 01184, 0 01184, 0 01184,
0 01184, 0 01184, 0 01184, 0 01184, 0 01184,
0 01184, 0 01184, 0 01184, 0 01184, 0 01184,
0 01184, 0 01184, 0 01184, 0 01184, 0 01184,
$ 
$NMODE DDISP =
0 00000, 0 00003, 0 00005, 0 00006, 0 00007,
0 00007, 0 00008, 0 00010, 0 00012, 0 00017,
0 00025, 0 00033, 0 00123, 0 00138, 0 00153,
0 00168, 0 00183, 0 00198, 0 00213, 0 00228,
0 00243, 0 00260, 0 00277, 0 00291, 0 00305,
0 00316, 0 00327, 0 00336, 0 00345, 0 00353,
0 00363, 0 00373, 0 00424, 0 00438, 0 00452,
0 00465, 0 00477, 0 00489, 0 00499,
DSLOP =
0 01184, 0 01184, 0 01184, 0 01184, 0 01184,
0 01184, 0 01184, 0 01184, 0 01184, 0 01184,
0 01184, 0 01184, 0 01184, 0 01184, 0 01184,
0 01184, 0 01184, 0 01184, 0 01184, 0 01184,
0 01184, 0 01184, 0 01184, 0 01184, 0 01184,
0 01184, 0 01184, 0 01184, 0 01184, 0 01184,
$ 
$NMODE DDISP =
0 00046, 0 00050, 0 00052, 0 00054, 0 00054,
0 00054, 0 00054, 0 00055, 0 00057, 0 00060,
0 00066, 0 00073, 0 00156, 0 00170, 0 00183,

```

```

0 00197, 0 00210, 0 00224, 0 00237, 0 00250.
0 00264, 0 00280, 0 00295, 0 00308, 0 00320.
0 00330, 0 00339, 0 00346, 0 00353, 0 00360.
0 00368, 0 00377, 0 00425, 0 00438, 0 00451.
0 00462, 0 00473, 0 00483, 0 00492.
DSLOP =
0 01184, 0 01184, 0 01184, 0 01184, 0 01184.
0 01184, 0 01184, 0 01184, 0 01184, 0 01184.
0 01184, 0 01184, 0 01184, 0 01184, 0 01184.
0 01184, 0 01184, 0 01184, 0 01184, 0 01184.
0 01184, 0 01184, 0 01184, 0 01184, 0 01184.
0 01184, 0 01184, 0 01184, 0 01184, 0 01184.
0 01184, 0 01184, 0 01184, 0 01184, 0 01184.
0 01184, 0 01184, 0 01184, 0 01184, 0 01184.
$  

$NMODE DDISP =
0 00084, 0 00088, 0 00090, 0 00091, 0 00092.
0 00091, 0 00091, 0 00091, 0 00092, 0 00094.
0 00099, 0 00105, 0 00183, 0 00196, 0 00208.
0 00220, 0 00232, 0 00244, 0 00256, 0 00268.
0 00281, 0 00296, 0 00309, 0 00321, 0 00332.
0 00341, 0 00349, 0 00355, 0 00360, 0 00366.
0 00372, 0 00380, 0 00426, 0 00438, 0 00449.
0 00460, 0 00470, 0 00479, 0 00487.
DSLOP =
0 01184, 0 01184, 0 01184, 0 01184, 0 01184.
0 01184, 0 01184, 0 01184, 0 01184, 0 01184.
0 01184, 0 01184, 0 01184, 0 01184, 0 01184.
0 01184, 0 01184, 0 01184, 0 01184, 0 01184.
0 01184, 0 01184, 0 01184, 0 01184, 0 01184.
0 01184, 0 01184, 0 01184, 0 01184, 0 01184.
0 01184, 0 01184, 0 01184, 0 01184, 0 01184.
$  

$NBUND DOWNST=4LSTEA,WINGBC=4LUNST, WAKEBC=4LUNST  $
$NANGL $
$NREFV SREF=2 9768, XMOMC=0 5,CREF=1 0,BREF=1 9468,XZERO=0 5,CBAR=1 0  $
$NVIS VISC= FALSE .WEDGE= FALSE ,GREEN= FALSE ,REYINF=10 0E7,IBLPRT=450 $
/EOF

```

\*\*\*\*\* SAMPLE OUTPUT FROM ATRAN3S \*\*\*\*\*

APPLIED COMPUTATIONAL AERODYNAMICS BRANCH  
NASA - AMES RESEARCH CENTER  
MOFFETT FIELD, CA 94035

PROGRAM ATRAN3S  
(THE AMES VERSION OF THE AIRFORCE-BOEING XTRAN3S)  
A UNSTEADY TRANSONIC AERODYNAMICS CODE FOR AEROELASTIC ANALYSIS OF WINGS

WRITTEN BY

DR GURU P GURUSWAMY  
(415) 694 6329

AND

DR PETER M GOORJIAN  
(415) 694 5547

1 CASE 370 M=0 9 K=0 275 (40HZ)

FLAGS TO CONTROL OUTPUT

DETAILED PRINT FLAG =	0
PRESSURE PRINT FREQUENCY =	1000
FORCE COEFFICIENT PRINT FREQUENCY =	1000
DISPLACEMENT PRINT FREQUENCY =	1
DISPLACEMENT PLOT DATA FREQUENCY =	1
NUMBER OF CYCLES OF INPUT SUPRESSION =	0

TASK = DYNAMIC ANALYSIS

FLOW PARAMETERS

FREE STREAM MACH NUMBER =	0 9000
FREE STREAM VELOCITY =	1 0000
RATIO OF SPECIFIC HEATS =	1 4000
TIME SCALE =	1 0000

COMPUTATION PARAMETERS

ITERATIONS COMPLETED =	0
------------------------	---

MAXIMUM STEADY ITERATIONS = 0  
 MAXIMUM UNSTEADY ITERATIONS = 3500  
 TIME ELAPSED = 0 000000  
 TIME STEP SIZE = 0 010000  
 0EQUATION PARAMETERS

EQUATION TYPE = MODIFIED SMALL DISTURBANCE  
 FREQUENCY = HIGH FREQUENCY APPROXIMATION  
 MODIFY = AMES COEFFICIENTS  
 1GRID SPECIFICATIONS

#### XI GRID

TOTAL NUMBER OF POINTS = 64  
 NUMBER OF POINTS FORWARD OF LE = 13  
 NUMBER OF POINTS ON WING = 39  
 NUMBER OF POINTS AFTER TE = 12  
 INDEX OF FIRST POINT ON WING = 14  
 LENGTH OF MESH IN FRONT OF LE = 15 37500  
 TOTAL LENGTH OF MESH = 41 95000  
 MESH SPACING AT LE = 0 01000  
 MESH SPACING AT TE = 0 02119  
 MAXIMUM MESH SPACING = 10 97436

#### ETA GRID

TOTAL NUMBER OF POINTS = 20  
 INDEX OF FIRST POINT = 1  
 NUMBER OF POINTS INBOARD OF WING TIP = 13  
 NUMBER OF POINTS OUTBOARD OF WING TIP = 7  
 TOTAL NUMBER OF MESHPOINTS ON WING = 13  
 TOTAL LENGTH OF MESH = 1 94680  
 LENGTH OF MESH INBOARD OF WING TIP = 0 95080  
 LENGTH OF MESH OUTBOARD OF WING TIP = 0 99600  
 MESH SPACING AT WING ROOT = 0 09730  
 MESH SPACING AT TIP = 0 04860  
 MAXIMUM MESH SPACING (AT FAR SPAN BOUNDARY) = 0 32300

#### ZETA GRID

TOTAL NUMBER OF ZETA GRID POINTS = 40  
 INDEX OF ZETA GRID POINT IMMEDIATELY ABOVE WING = 21  
 INDEX OF ZETA GRID POINT IMMEDIATELY BELOW WING = 20  
 NUMBER OF ZETA GRID POINTS BELOW WING = 20  
 NUMBER OF ZETA GRID POINTS ABOVE WING = 20  
 TOTAL LENGTH OF MESH = 49 82800  
 LENGTH OF MESH ABOVE WING = 24 91400  
 LENGTH OF MESH BELOW WING = 24 91400  
 SPACING AT UPPER BOUNDARY = 11 23900  
 SPACING AT LOWER BOUNDARY = 11 23900  
 SPACING AT WING = 0 02000

#### 1GRID POINTS

INDEX	XI	INDEX	ETA	INDEX	ZETA
1	-15 37500	1	-0 09730	1	-24 91400
2	-8 10791	2	0 00000	2	-13 67500
3	-4 24734	3	0 09730	3	-7.72800

4	-2	20500	4	0.19470	4	-4	50200
5	-1	13177	5	0 29200	5	-2	70600
6	-0	57371	6	0 38940	6	-1	68000
7	-0	28812	7	0 48670	7	-1	07800
8	-0	14526	8	0 58350	8	-0	71400
9	-0	07579	9	0 67800	9	-0	48800
10	-0	04260	10	0 76590	10	-0	34400
11	-0	02589	11	0 84150	11	-0	24800
12	-0	01506	12	0 90220	12	-0	18400
13	-0	00500	13	0 95080	13	-0	13800
14	0	00500	14	0 99380	14	-0	10500
15	0	01506	15	1 03940	15	-0	08000
16	0	02539	16	1 10020	16	-0	06100
17	0	03653	17	1 19880	17	-0	04500
18	0	04938	18	1.36690	18	-0	03200
19	0	06493	19	1 62380	19	-0	02000
20	0	08391	20	1 94680	20	-0	01000
21	0	10654			21	0	01000
22	0	13245			22	0	02000
23	0	16067			23	0	03200
24	0	19012			24	0	04500
25	0	22001			25	0	06100
26	0	25000			26	0	08000
27	0	28000			27	0	10500
28	0	31000			28	0	13800
29	0	34000			29	0	18400
30	0	37000			30	0	24800
31	0	40000			31	0	34400
32	0	43000			32	0	48800
33	0	46000			33	0	71400
34	0	49000			34	1	07800
35	0	52000			35	1	68000
36	0	55000			36	2	70600
37	0	58000			37	4	50200
38	0	61000			38	7	72800
39	0	64000			39	13	67500
40	0	67000			40	24.91400	
41	0	70000					
42	0	73000					
43	0	76000					
44	0	79000					
45	0	81994					
46	0	84966					
47	0	87875					
48	0	90659					
49	0	93262					
50	0	95660					
51	0	97881					
52	1	00000					
53	1	02188					
54	1	05155					
55	1	10369					
56	1	20357					
57	1	39472					
58	1	75209					
59	2	40476					
60	3	57502					
61	5	64564					
62	9	27579					
63	15	60064					

64 26.57500

PLANFORM DESCRIPTION

FORMAT =	RATIO
ASPECT RATIO =	2 98
TAPER RATIO =	0 31
SWEET ANGLE (DEGREES) =	31 92
NUMBER OF AIRFOIL SECTIONS =	2

INPUT IS IN THE FORM OF SLOPES  
1 INPUT AIRFOIL GEOMETRY FOR SECTION NO = 1 AT ETA = 0 00000

UPPER SURFACE

LOWER SURFACE

INDEX	X	Z	INDEX	X	Z
1	0 00500	0 31365	1	0 00500	-0 27687
2	0 01500	0 23291	2	0 01500	-0 11999
3	0 02500	0 20255	3	0 02500	-0 07540
4	0 03500	0 18295	4	0 03500	-0 05394
5	0 04500	0 16790	5	0 04500	-0 04169
6	0 06000	0 14974	6	0 06000	-0 03137
7	0 08000	0 13017	7	0 08000	-0 02474
8	0 10000	0 11384	8	0 10000	-0 02184
9	0 13000	0 09336	9	0 13000	-0 02041
10	0 16000	0 07637	10	0 16000	-0 02020
11	0 19000	0 06202	11	0 19000	-0 02009
12	0 22000	0 04978	12	0 22000	-0 01960
13	0 25000	0 03925	13	0 25000	-0 01852
14	0 28000	0 03012	14	0 28000	-0 01677
15	0 31000	0 02214	15	0 31000	-0 01438
16	0 34000	0 01508	16	0 34000	-0 01137
17	0 37000	0 00875	17	0 37000	-0 00780
18	0 40000	0 00300	18	0 40000	-0 00377
19	0 43000	-0 00233	19	0 43000	0 00065
20	0 46000	-0 00733	20	0 46000	0 00537
21	0 49000	-0 01212	21	0 49000	0 01030
22	0 52000	-0 01676	22	0 52000	0 01537
23	0 55000	-0 02130	23	0 55000	0 02049
24	0 58000	-0 02580	24	0 58000	0 02558
25	0 61000	-0 03026	25	0 61000	0 03056
26	0 64000	-0 03469	26	0 64000	0 03538
27	0 67000	-0 03905	27	0 67000	0 03997
28	0 70000	-0 04333	28	0 70000	0 04427
29	0 73000	-0 04745	29	0 73000	0 04823
30	0 76000	-0 05134	30	0 76000	0 05181
31	0 79000	-0 05492	31	0 79000	0 05496
32	0 82000	-0 05806	32	0 82000	0 05765
33	0 85000	-0 06065	33	0 85000	0 05986
34	0 88000	-0 06252	34	0 88000	0 06157
35	0 91000	-0 06352	35	0 91000	0 06275
36	0 93500	-0 06356	36	0 93500	0 06334
37	0 96000	-0 06274	37	0 96000	0 06356
38	0 98000	-0 06139	38	0 98000	0 06348

39 1 00000 -0 05935 39 1 00000 0 06316  
 1 INPUT AIRFOIL GEOMETRY FOR SECTION NO = 2 AT ETA = 0 97340

UPPER SURFACE

LOWER SURFACE

INDEX	X	Z	INDEX	X	Z
1	0 00500	0 31365	1	0 00500	-0 27687
2	0 01500	0 23291	2	0 01500	-0 11999
3	0 02500	0 20255	3	0 02500	-0 07540
4	0 03500	0 18295	4	0 03500	-0 05394
5	0 04500	0 16790	5	0 04500	-0 04169
6	0 06000	0 14974	6	0 06000	-0 03137
7	0 08000	0 13017	7	0 08000	-0 02474
8	0 10000	0 11384	8	0 10000	-0 02184
9	0 13000	0 09336	9	0 13000	-0 02041
10	0 16000	0 07637	10	0 16000	-0 02020
11	0 19000	0 06202	11	0 19000	-0 02009
12	0 22000	0 04978	12	0 22000	-0 01960
13	0 25000	0 03925	13	0 25000	-0 01852
14	0 28000	0 03012	14	0 28000	-0 01677
15	0 31000	0 02214	15	0 31000	-0 01438
16	0 34000	0 01508	16	0 34000	-0 01137
17	0 37000	0 00875	17	0 37000	-0 00780
18	0 40000	0 00300	18	0 40000	-0 00377
19	0 43000	-0 00233	19	0 43000	0 00065
20	0 46000	-0 00733	20	0 46000	0 00537
21	0 49000	-0 01212	21	0 49000	0 01030
22	0 52000	-0 01676	22	0 52000	0 01537
23	0 55000	-0 02130	23	0 55000	0 02049
24	0 58000	-0 02580	24	0 58000	0 02558
25	0 61000	-0 03026	25	0 61000	0 03056
26	0 64000	-0 03469	26	0 64000	0 03538
27	0 67000	-0 03905	27	0 67000	0 03997
28	0 70000	-0 04333	28	0 70000	0 04427
29	0 73000	-0 04745	29	0 73000	0 04823
30	0 76000	-0 05134	30	0 76000	0 05181
31	0 79000	-0 05492	31	0 79000	0 05496
32	0 82000	-0 05806	32	0 82000	0 05765
33	0 85000	-0 06065	33	0 85000	0 05986
34	0 88000	-0 06252	34	0 88000	0 06157
35	0 91000	-0 06352	35	0 91000	0 06275
36	0 93500	-0 06356	36	0 93500	0 06334
37	0 96000	-0 06274	37	0 96000	0 06356
38	0 98000	-0 06139	38	0 98000	0 06348
39	1 00000	-0 05935	39	1 00000	0 06316

1AIRFOIL SURFACE SLOPES - UPPER SURFACE

INDEX	XI	SPAN STATIONS/ETA												
		1/ -0 10	2/ 0 00	3/ 0 10	4/ 0 19	5/ 0 29	6/ 0 39	7/ 0 49	8/ 0 58	9/ 0 68	10/ 0 77	11/ 0 84	12/ 0 90	13/ 0 95
1	0 005	0 314	0 314	0 314	0 314	0 314	0 314	0 314	0 314	0 314	0 314	0 314	0 314	
2	0 015	0 233	0 233	0 233	0 233	0 233	0 233	0 233	0 233	0 233	0 233	0 233	0 233	
3	0 025	0 203	0 203	0 203	0 203	0 203	0 203	0 203	0 203	0 203	0 203	0 203	0 203	
4	0 037	0 183	0 183	0 183	0 183	0 183	0 183	0 183	0 183	0 183	0 183	0 183	0 183	
5	0 049	0 168	0 168	0 168	0 168	0 168	0 168	0 168	0 168	0 168	0 168	0 168	0 168	
6	0 065	0 150	0 150	0 150	0 150	0 150	0 150	0 150	0 150	0 150	0 150	0 150	0 150	
7	0 084	0 130	0 130	0 130	0 130	0 130	0 130	0 130	0 130	0 130	0 130	0 130	0 130	
8	0 107	0 114	0 114	0 114	0 114	0 114	0 114	0 114	0 114	0 114	0 114	0 114	0 114	

29 39 1 000 -0.059 -0.059 -0.059 1AIRFOIL SURFACE SLOPES - LOWER SURFACE

SPAN STATIONS/ETA

## 1 MOTION DESCRIPTION

MODAL LIFE

FREQUENCY = 0 55000

卷之三

NUMBER OF TIME STEPS PER CYCLE = 1142  
DISPLACEMENTS FOR ALL GRID POINTS ON WING

1SLOPES FOR ALL GRID POINTS ON WING

## 1 BOUNDARY CONDITION DATA

DOWNTSTREAM BOUNDARY CONDITION STEADY  
(FREQUENCY = LOW)

UPSTREAM BOUNDARY CONDITION FREESTREAM

FARFIELD BOUNDARY CONDITION FREEJET

VELOCITY AT LOWER BOUNDARY = 0 0

VELOCITY AT UPPER BOUNDARY = 0 0

JUMP CONDITION ACROSS WAKE UNSTEADY

WIND TUNNEL WALLS NOT USED AS BOUNDARIES

LIFTING SURFACE UNSTEADY

ANGLES OF ATTACK

RIGID ANGLE OF ATTACK (DEG) = 0 00000

TWIST IN DEGREES

SPAN = -0 097 0 000 0 097 0 195 0 292 0 389 0 487 0 584 0 678 0 766 0 841 0 902 0 951

TWIST = 0 000 0 000 0 000 0 000 0 000 0 000 0 000 0 000 0 000 0 000 0 000 0 000 0 000

REFERENCE AREA = 2 97680

MEAN AERODYNAMIC CHORD = 1 00000

32

MOMENT CENTER REFERENCE = 0 50000

REFERENCE CHORD = 1 00000

REFERENCE SPAN = 1 94680

1 MOMENT REFERENCE VARIABLE = 0 50000  
PHYSICAL X GRID

INDEX	XI	SPAN STATIONS/ETA									
		-0 10	0 00	0 10	0 19	0 29	0 39	0 49	0 58	0 68	0 77
1	-15 375	-15 000	-15 000	-15 000	-15 000	-15 000	-15 000	-15 000	-15 000	-15 000	-15 000
2	-8 108	-8 012	-7 929	-7 842	-7 751	-7 655	-7 554	-7 445	-7 328	-7 205	-7 079
3	-4 247	-4 264	-4 163	-4 059	-3 951	-3 839	-3 721	-3 596	-3 465	-3 329	-3 192
4	-2 205	-2 262	-2 166	-2 068	-1 967	-1 863	-1 755	-1 643	-1 527	-1 408	-1 291
5	-1 132	-1 201	-1 115	-1 027	-0 937	-0 846	-0 753	-0 657	-0 559	-0 460	-0 365
6	-0 574	-0 644	-0 566	-0 488	-0 408	-0 328	-0 247	-0 164	-0 081	0 002	0 081
7	-0 288	-0 357	-0 285	-0 213	-0 141	-0 068	0 005	0 078	0 152	0 225	0 294
8	-0 145	-0 212	-0 144	-0 077	-0 009	0 059	0 127	0 195	0 263	0 330	0 393
9	-0 076	-0 140	-0 075	-0 011	0 054	0 119	0 185	0 250	0 315	0 378	0 437
10	-0 043	-0 106	-0 043	0 021	0 084	0 148	0 211	0 274	0 338	0 399	0 456
11	-0 026	-0 088	-0 026	0 036	0 099	0 161	0 224	0 286	0 348	0 409	0 465
12	-0 015	-0 077	-0 015	0 047	0 108	0 170	0 232	0 293	0 355	0 414	0 470
13	-0 005	-0 066	-0 005	0 056	0 117	0 178	0 239	0 300	0 361	0 420	0 475
14	0 005	-0 055	0 005	0 065	0 126	0 186	0 246	0 306	0 366	0 425	0 479
15	0 015	-0 045	0 015	0 075	0 134	0 194	0 253	0 313	0 372	0 430	0 484
16	0 025	-0 033	0 025	0 084	0 143	0 202	0 261	0 320	0 378	0 435	0 489
17	0 037	-0 022	0 037	0 095	0 153	0 211	0 269	0 327	0 385	0 441	0 494
18	0 049	-0 008	0 049	0 107	0 164	0 221	0 278	0 335	0 392	0 448	0 500

19	0 065	0 009	0 065	0 121	0 177	0 233	0 289	0 346	0 401	0 456	0 507
20	0 084	0 029	0 084	0 139	0 194	0 248	0 303	0 358	0 413	0 466	0 515
21	0 107	0 053	0 107	0 160	0 213	0 266	0 320	0 373	0 426	0 477	0 526
22	0 132	0 081	0 132	0 184	0 235	0 287	0 338	0 390	0 441	0 491	0 537
23	0 161	0 111	0 161	0 210	0 260	0 309	0 359	0 408	0 457	0 506	0 550
24	0 190	0 143	0 190	0 238	0 285	0 333	0 380	0 427	0 475	0 521	0 564
25	0 220	0 175	0 220	0 265	0 311	0 356	0 402	0 447	0 492	0 536	0 577
26	0 250	0 207	0 250	0 293	0 337	0 380	0 423	0 467	0 510	0 552	0 591
27	0 280	0 239	0 280	0 321	0 363	0 404	0 445	0 486	0 527	0 567	0 605
28	0 310	0 271	0 310	0 349	0 388	0 428	0 467	0 506	0 545	0 583	0 618
29	0 340	0 303	0 340	0 377	0 414	0 451	0 488	0 526	0 562	0 598	0 632
30	0 370	0 335	0 370	0 405	0 440	0 475	0 510	0 545	0 580	0 614	0 646
31	0 400	0 367	0 400	0 433	0 466	0 499	0 532	0 565	0 598	0 630	0 659
32	0 430	0 399	0 430	0 461	0 492	0 523	0 554	0 584	0 615	0 645	0 673
33	0 460	0 431	0 460	0 489	0 518	0 546	0 575	0 604	0 633	0 661	0 687
34	0 490	0 463	0 490	0 517	0 543	0 570	0 597	0 624	0 650	0 676	0 700
35	0 520	0 495	0 520	0 545	0 569	0 594	0 619	0 643	0 668	0 692	0 714
36	0 550	0 527	0 550	0 573	0 595	0 618	0 640	0 663	0 685	0 707	0 728
37	0 580	0 560	0 580	0 600	0 621	0 641	0 662	0 682	0 703	0 723	0 741
38	0 610	0 592	0 610	0 628	0 647	0 665	0 684	0 702	0 720	0 738	0 755
39	0 640	0 624	0 640	0 656	0 673	0 689	0 705	0 722	0 738	0 754	0 769
40	0 670	0 656	0 670	0 684	0 699	0 713	0 727	0 741	0 756	0 769	0 782

1

INDEX	XI	SPAN STATIONS/ETA									
		11/ 0 84	12/ 0 90	13/ 0 95	14/ 0 99	15/ 1 04	16/ 1 10	17/ 1 20	18/ 1 37	19/ 1 62	20/ 1 95
1	-15 375	-15 000	-15 000	-15 000	-15 000	-15 000	-15 000	-15 000	-15 000	-15 000	
2	-8 108	-6 960	-6 855	-6 764	-6 685	-6 613	-6 542	-6 496	-6 473	-6 437	
3	-4 247	-3 065	-2 956	-2 862	-2 782	-2 709	-2 636	-2 585	-2 552	-2 501	
4	-2 205	-1 184	-1 094	-1 018	-0 954	-0 895	-0 836	-0 790	-0 753	-0 695	
5	-1 132	-0 280	-0 209	-0 151	-0 101	-0 056	-0 009	0 030	0 070	0 129	
6	-0 574	0 151	0 208	0 254	0 294	0 329	0 367	0 403	0 443	0 504	
7	-0 288	0 353	0 402	0 441	0 474	0 504	0 537	0 570	0 610	0 671	
8	-0 145	0 447	0 490	0 525	0 554	0 581	0 611	0 643	0 683	0 745	
9	-0 076	0 488	0 529	0 562	0 589	0 615	0 643	0 674	0 714	0 776	
10	-0 043	0 506	0 545	0 577	0 604	0 628	0 656	0 687	0 727	0 788	
11	-0 026	0 514	0 553	0 584	0 610	0 634	0 661	0 692	0 732	0 794	
12	-0 015	0 518	0 557	0 587	0 613	0 637	0 664	0 695	0 735	0 796	
13	-0 005	0 522	0 560	0 591	0 616	0 640	0 667	0 697	0 737	0 799	
14	0 005	0 526	0 564	0 594	0 619	0 643	0 669	0 700	0 740	0 801	
15	0 015	0 530	0 567	0 597	0 622	0 645	0 672	0 702	0 742	0 804	
16	0 025	0 534	0 571	0 600	0 625	0 648	0 674	0 705	0 745	0 806	
17	0 037	0 539	0 575	0 604	0 628	0 651	0 677	0 707	0 748	0 809	
18	0 049	0 544	0 580	0 608	0 632	0 655	0 680	0 710	0 751	0 812	
19	0 065	0 550	0 585	0 613	0 637	0 659	0 684	0 714	0 754	0 816	
20	0 084	0 558	0 592	0 619	0 642	0 664	0 689	0 719	0 759	0 820	
21	0 107	0 567	0 600	0 627	0 649	0 670	0 695	0 724	0 765	0 826	
22	0 132	0 577	0 609	0 635	0 657	0 677	0 701	0 731	0 771	0 832	
23	0 161	0 589	0 620	0 644	0 665	0 685	0 708	0 738	0 778	0 839	
24	0 190	0 601	0 630	0 654	0 674	0 693	0 716	0 745	0 785	0 846	
25	0 220	0 613	0 641	0 664	0 683	0 701	0 723	0 752	0 792	0 854	
26	0 250	0 625	0 652	0 673	0 692	0 710	0 731	0 759	0 799	0 861	
27	0 280	0 637	0 662	0 683	0 701	0 718	0 739	0 767	0 807	0 868	
28	0 310	0 649	0 673	0 693	0 709	0 726	0 746	0 774	0 814	0 875	
29	0 340	0 661	0 684	0 702	0 718	0 734	0 754	0 781	0 821	0 883	
30	0 370	0 673	0 695	0 712	0 727	0 742	0 761	0 788	0 829	0 890	
31	0 400	0 685	0 705	0 722	0 736	0 751	0 769	0 796	0 836	0 897	
32	0 430	0 697	0 716	0 732	0 745	0 759	0 777	0 803	0 843	0 905	
33	0 460	0 709	0 727	0 741	0 754	0 767	0 784	0 810	0 850	0 912	

33

34	0 490	0 721	0 738	0 751	0 763	0 775	0 792	0 818	0 858	0 919	0 996
35	0 520	0 733	0 748	0 761	0 772	0 783	0 799	0 825	0 865	0 926	1 004
36	0 550	0 745	0 759	0 770	0 781	0 792	0 807	0 832	0 872	0 934	1 011
37	0 580	0 757	0 770	0 780	0 789	0 800	0 814	0 839	0 880	0 941	1 018
38	0 610	0 769	0 781	0 790	0 798	0 808	0 822	0 847	0 887	0 948	1 026
39	0 640	0 781	0 791	0 800	0 807	0 816	0 830	0 854	0 894	0 956	1 033
40	0 670	0 793	0 802	0 809	0 816	0 824	0 837	0 861	0 901	0 963	1 040

1

INDEX	XI	SPAN STATIONS/ETA									
		1/ -0	1/ 10	2/ 0	3/ 0	4/ 10	5/ 0	6/ 29	7/ 0	8/ 49	9/ 0
41	0 700	0 688	0 700	0 712	0 724	0 737	0 749	0 761	0 773	0 785	0 796
42	0 730	0 720	0 730	0 740	0 750	0 760	0 770	0 781	0 791	0 800	0 810
43	0 760	0 752	0 760	0 768	0 776	0 784	0 792	0 800	0 808	0 816	0 823
44	0 790	0 784	0 790	0 796	0 802	0 808	0 814	0 820	0 826	0 832	0 837
45	0 820	0 816	0 820	0 824	0 828	0 832	0 836	0 839	0 843	0 847	0 851
46	0 850	0 848	0 850	0 851	0 853	0 855	0 857	0 859	0 861	0 862	0 864
47	0 879	0 879	0 879	0 879	0 878	0 878	0 878	0 878	0 878	0 877	0 877
48	0 907	0 909	0 907	0 904	0 902	0 900	0 898	0 896	0 894	0 892	0 890
49	0 933	0 937	0 933	0 929	0 925	0 921	0 917	0 913	0 909	0 905	0 902
50	0 957	0 962	0 957	0 951	0 945	0 940	0 934	0 929	0 923	0 918	0 913
51	0 979	0 986	0 979	0 972	0 965	0 958	0 950	0 943	0 936	0 929	0 923
52	1 000	1 009	1 000	0 991	0 983	0 974	0 966	0 957	0 949	0 940	0 933
53	1 022	1 032	1 022	1 012	1 002	0 992	0 982	0 971	0 961	0 952	0 943
54	1 052	1 064	1 052	1 039	1 027	1 015	1 003	0 991	0 979	0 967	0 956
55	1 104	1 102	1 087	1 073	1 058	1 044	1 029	1 015	1 000	0 986	0 973
56	1 204	1 166	1 148	1 130	1 112	1 094	1 075	1 057	1 039	1 021	1 004
57	1 395	1 289	1 265	1 241	1 217	1 193	1 168	1 144	1 119	1 094	1 071
58	1 752	1 529	1 496	1 463	1 429	1 395	1 361	1 325	1 289	1 254	1 219
59	2 405	1 995	1 949	1 902	1 854	1 804	1 753	1 701	1 647	1 592	1 539
60	3 575	2 892	2 827	2 759	2 690	2 618	2 542	2 464	2 382	2 298	2 215
61	5 646	4 595	4 506	4 414	4 317	4 216	4 110	3 997	3 878	3 753	3 628
62	9 276	7 802	7 693	7 579	7 458	7 330	7 194	7 048	6 892	6 726	6 557
63	15 601	13 805	13 704	13 597	13 483	13 361	13 230	13 088	12 933	12 766	12 594
64	26 575	25 000	25 000	25 000	25 000	25 000	25 000	25 000	25 000	25 000	25 000

34

INDEX	XI	SPAN STATIONS/ETA									
		11/ 0	12/ 84	13/ 0	14/ 95	15/ 99	16/ 1	17/ 10	18/ 1	19/ 37	19/ 62
41	0 700	0 805	0 813	0 819	0 825	0 833	0 845	0 869	0 909	0 970	1 047
42	0 730	0 817	0 824	0 829	0 834	0 841	0 852	0 876	0 916	0 977	1 055
43	0 760	0 829	0 834	0 839	0 843	0 849	0 860	0 883	0 923	0 985	1 062
44	0 790	0 842	0 845	0 848	0 852	0 857	0 867	0 890	0 931	0 992	1 069
45	0 820	0 854	0 856	0 858	0 861	0 865	0 875	0 898	0 938	0 999	1 077
46	0 850	0 866	0 867	0 868	0 869	0 874	0 883	0 905	0 945	1 007	1 084
47	0 879	0 877	0 877	0 877	0 878	0 881	0 890	0 912	0 952	1 014	1 091
48	0 907	0 888	0 887	0 886	0 886	0 889	0 897	0 919	0 959	1 020	1 098
49	0 933	0 899	0 896	0 894	0 894	0 896	0 904	0 925	0 965	1 027	1 104
50	0 957	0 908	0 905	0 902	0 901	0 903	0 910	0 931	0 971	1 033	1 110
51	0 979	0 917	0 913	0 909	0 908	0 909	0 915	0 936	0 977	1 038	1 115
52	1 000	0 926	0 921	0 916	0 914	0 915	0 921	0 942	0 982	1 043	1 120
53	1 022	0 935	0 928	0 923	0 920	0 921	0 926	0 947	0 987	1 048	1 126
54	1 052	0 947	0 939	0 933	0 929	0 929	0 934	0 954	0 994	1 056	1 133
55	1 104	0 961	0 952	0 945	0 940	0 939	0 943	0 963	1 003	1 065	1 142
56	1 204	0 990	0 978	0 968	0 962	0 959	0 962	0 982	1 022	1 083	1 160
57	1 395	1 051	1 035	1 022	1 012	1 007	1 007	1 025	1 065	1 127	1 204
58	1 752	1 189	1 164	1 144	1 128	1 117	1 113	1 129	1 169	1 230	1 307

59	2 405	1 491	1 451	1 417	1.391	1 370	1 357	1 368	1 408	1.469	1 546
60	3 575	2 139	2 074	2 019	1 974	1 938	1 909	1 913	1 952	2 012	2 087
61	5 646	3 512	3 411	3 325	3 253	3 192	3 139	3 130	3 168	3 226	3 298
62	9 276	6 397	6 257	6 135	6 031	5 941	5 859	5 835	5 869	5 921	5 986
63	15 601	12 428	12 281	12 151	12 039	11 940	11 848	11 814	11 838	11 875	11 921
64	26 575	25 000	25 000	25 000	25 000	25 000	25 000	25 000	25 000	25 000	25 000

PLAN FORM COMPUTED FROM GDPLAN

SPAN	STATION	ETA	XLE	XTE	CHORD
1		-0 0973	-0 0606	1 0086	1 0692
2		0 0000	0 0000	1 0000	1 0000
3		0 0973	0 0606	0 9914	0 9308
4		0 1947	0 1213	0 9829	0 8616
5		0 2920	0 1819	0 9743	0 7924
6		0 3894	0 2425	0 9657	0 7232
7		0 4867	0 3031	0 9571	0 6540
8		0 5835	0 3634	0 9486	0 5852
9		0 6780	0 4223	0 9403	0 5180
10		0 7659	0 4770	0 9326	0 4555
11		0 8415	0 5241	0 9259	0 4018
12		0 9022	0 5619	0 9206	0 3586
13		0 9508	0 5922	0 9163	0 3241
14		0 9938	0 6176	0 9139	0 2964
15		1 0394	0 6413	0 9146	0 2733
16		1 1002	0 6679	0 9205	0 2527
17		1 1988	0 6985	0 9415	0 2431
18		1 3669	0 7386	0 9817	0 2431
19		1 6238	0 8001	1 0431	0 2431
20		1 9468	0 8773	1 1203	0 2431

TOTAL AREA IN USERS UNITS = 0 62632

\*\*\*\*\* Note Results for cycle 1 and 2 are skipped \*\*\*\*\*

CYCLE = 3

OURIER COEFFICIENTS FOR UPPER SURFACE PRESSURES CONSTANT TERM (A0)

INDEX	XI	SPAN STATIONS/ETA												
		1/ -0 10	2/ 0 00	3/ 0 10	4/ 0 19	5/ 0 29	6/ 0 39	7/ 0 49	8/ 0 58	9/ 0 68	10/ 0 77	11/ 0 84	12/ 0 90	13/ 0 95
1	0 005	2 838	0 717	0 541	0 522	0 514	0 505	0 494	0 481	0 467	0 450	0 430	0 404	0 324
2	0 015	2 492	0 534	0 393	0 374	0 364	0 356	0 348	0 339	0 329	0 317	0 303	0 279	0 192
3	0 025	1 881	0 382	0 274	0 252	0 241	0 233	0 226	0 218	0 211	0 203	0 193	0 169	0 076
4	0 037	1 153	0 280	0 196	0 171	0 158	0 148	0 140	0 132	0 125	0 117	0 107	0 081	-0 016
5	0 049	0 728	0 204	0 130	0 104	0 088	0 077	0 067	0 058	0 050	0 042	0 031	0 000	-0 098
6	0 065	0 495	0 137	0 070	0 042	0 025	0 012	0 001	-0 009	-0 018	-0 028	-0 041	-0 078	-0 172
7	0 084	0 314	0 081	0 019	-0 010	-0 029	-0 044	-0 056	-0 067	-0 077	-0 089	-0 106	-0 149	-0 232
8	0 107	0 196	0 029	-0 029	-0 059	-0 080	-0 096	-0 109	-0 121	-0 133	-0 146	-0 169	-0 217	-0 278
9	0 132	0 110	-0 019	-0 071	-0 102	-0 123	-0 140	-0 154	-0 167	-0 180	-0 196	-0 223	-0 272	-0 309
10	0 161	0 026	-0 056	-0 101	-0 131	-0 152	-0 170	-0 185	-0 199	-0 214	-0 232	-0 263	-0 307	-0 321
11	0 190	-0 029	-0 086	-0 126	-0 154	-0 175	-0 193	-0 209	-0 223	-0 239	-0 260	-0 292	-0 330	-0 322
12	0 220	-0 068	-0 111	-0 146	-0 172	-0 193	-0 211	-0 226	-0 241	-0 258	-0 281	-0 315	-0 343	-0 314
13	0 250	-0 100	-0 132	-0 163	-0 187	-0 207	-0 224	-0 240	-0 255	-0 273	-0 298	-0 331	-0 347	-0 301
14	0 280	-0 126	-0 150	-0 177	-0 199	-0 218	-0 235	-0 250	-0 266	-0 285	-0 312	-0 341	-0 343	-0 283
15	0 310	-0 147	-0 166	-0 189	-0 209	-0 227	-0 243	-0 258	-0 274	-0 295	-0 322	-0 345	-0 331	-0 263
16	0 340	-0 165	-0 179	-0 199	-0 218	-0 234	-0 249	-0 264	-0 281	-0 302	-0 328	-0 342	-0 313	-0 241
17	0 370	-0 180	-0 191	-0 208	-0 225	-0 240	-0 255	-0 270	-0 287	-0 308	-0 330	-0 333	-0 289	-0 220
18	0 400	-0 192	-0 202	-0 217	-0 231	-0 246	-0 259	-0 274	-0 291	-0 311	-0 328	-0 317	-0 262	-0 200
19	0 430	-0 204	-0 211	-0 224	-0 237	-0 250	-0 263	-0 277	-0 294	-0 312	-0 321	-0 294	-0 234	-0 182
20	0 460	-0 213	-0 220	-0 231	-0 243	-0 254	-0 266	-0 280	-0 295	-0 310	-0 308	-0 266	-0 208	-0 169
21	0 490	-0 222	-0 227	-0 237	-0 247	-0 257	-0 268	-0 281	-0 294	-0 303	-0 287	-0 233	-0 187	-0 158
22	0 520	-0 230	-0 234	-0 241	-0 250	-0 259	-0 269	-0 280	-0 290	-0 290	-0 257	-0 201	-0 172	-0 149
23	0 550	-0 236	-0 238	-0 244	-0 251	-0 259	-0 267	-0 275	-0 280	-0 265	-0 216	-0 177	-0 162	-0 142
24	0 580	-0 241	-0 241	-0 245	-0 249	-0 255	-0 261	-0 264	-0 258	-0 225	-0 178	-0 163	-0 154	-0 134
25	0 610	-0 242	-0 240	-0 241	-0 243	-0 245	-0 245	-0 239	-0 216	-0 176	-0 156	-0 154	-0 145	-0 125
26	0 640	-0 238	-0 232	-0 229	-0 226	-0 221	-0 212	-0 192	-0 164	-0 145	-0 146	-0 144	-0 134	-0 115
27	0 670	-0 222	-0 211	-0 201	-0 190	-0 178	-0 162	-0 144	-0 133	-0 134	-0 135	-0 131	-0 122	-0 104
28	0 700	-0 190	-0 172	-0 157	-0 145	-0 134	-0 124	-0 119	-0 119	-0 120	-0 119	-0 115	-0 107	-0 092
29	0 730	-0 150	-0 131	-0 119	-0 112	-0 107	-0 104	-0 102	-0 101	-0 100	-0 099	-0 097	-0 091	-0 079
30	0 760	-0 111	-0 099	-0 092	-0 088	-0 084	-0 082	-0 080	-0 078	-0 078	-0 077	-0 076	-0 073	-0 064
31	0 790	-0 078	-0 069	-0 064	-0 061	-0 058	-0 056	-0 054	-0 053	-0 052	-0 052	-0 053	-0 052	-0 047
32	0 820	-0 044	-0 038	-0 034	-0 031	-0 029	-0 027	-0 026	-0 025	-0 024	-0 025	-0 027	-0 029	-0 029
33	0 850	-0 008	-0 004	-0 002	0 000	0 002	0 004	0 005	0 006	0 006	0 004	0 001	-0 004	-0 008
34	0 879	0 030	0 031	0 032	0 033	0 035	0 036	0 037	0 038	0 038	0 036	0 032	0 024	0 014
35	0 907	0 069	0 066	0 066	0 067	0 068	0 070	0 071	0 071	0 071	0 069	0 064	0 055	0 039
36	0 933	0 109	0 102	0 101	0 102	0 103	0 104	0 105	0 106	0 105	0 103	0 098	0 088	0 067
37	0 957	0 153	0 140	0 138	0 139	0 140	0 141	0 142	0 142	0 142	0 140	0 135	0 124	0 099
38	0 979	0 208	0 185	0 182	0 183	0 184	0 186	0 186	0 187	0 187	0 185	0 180	0 168	0 141
39	1 000	0 315	0 263	0 260	0 260	0 261	0 261	0 261	0 260	0 258	0 255	0 248	0 236	0 208

## FOURIER COEFFICIENTS FOR UPPER SURFACE PRESSURES A1 TERM

CYCLE = 3

INDEX	XI	SPAN STATIONS/ETA												
		1/ -0 10	2/ 0 00	3/ 0 10	4/ 0 19	5/ 0 29	6/ 0 39	7/ 0 49	8/ 0 58	9/ 0 68	10/ 0 77	11/ 0 84	12/ 0 90	13/ 0 95
1	0 005	-0 030	-0 021	-0 026	-0 031	-0 035	-0 038	-0 041	-0 044	-0 046	-0 048	-0 049	-0 049	-0 045
2	0 015	-0 042	-0 018	-0 022	-0 027	-0 030	-0 033	-0 036	-0 039	-0 042	-0 044	-0 046	-0 046	-0 042
3	0 025	-0 043	-0 016	-0 019	-0 023	-0 026	-0 029	-0 032	-0 035	-0 038	-0 041	-0 042	-0 043	-0 039
4	0 037	-0 033	-0 014	-0 017	-0 020	-0 023	-0 026	-0 028	-0 031	-0 035	-0 037	-0 039	-0 040	-0 035
5	0 049	-0 025	-0 013	-0 015	-0 018	-0 020	-0 023	-0 026	-0 029	-0 032	-0 034	-0 036	-0 037	-0 033
6	0 065	-0 020	-0 012	-0 013	-0 016	-0 018	-0 021	-0 023	-0 026	-0 029	-0 032	-0 034	-0 035	-0 030
7	0 084	-0 016	-0 011	-0 012	-0 014	-0 016	-0 019	-0 021	-0 024	-0 027	-0 030	-0 032	-0 033	-0 026
8	0 107	-0 014	-0 010	-0 011	-0 013	-0 015	-0 017	-0 020	-0 023	-0 026	-0 029	-0 031	-0 031	-0 023
9	0 132	-0 012	-0 010	-0 010	-0 012	-0 014	-0 016	-0 019	-0 022	-0 025	-0 028	-0 029	-0 027	-0 021
10	0 161	-0 011	-0 009	-0 009	-0 010	-0 012	-0 015	-0 018	-0 021	-0 024	-0 026	-0 027	-0 025	-0 019
11	0 190	-0 010	-0 008	-0 008	-0 009	-0 011	-0 014	-0 016	-0 019	-0 022	-0 024	-0 025	-0 024	-0 017
12	0 220	-0 011	-0 007	-0 006	-0 008	-0 010	-0 012	-0 015	-0 018	-0 020	-0 022	-0 024	-0 022	-0 014
13	0 250	-0 009	-0 006	-0 006	-0 007	-0 009	-0 012	-0 014	-0 017	-0 020	-0 022	-0 023	-0 020	-0 011
14	0 280	-0 006	-0 006	-0 007	-0 008	-0 010	-0 013	-0 015	-0 018	-0 021	-0 023	-0 024	-0 019	-0 008
15	0 310	-0 006	-0 006	-0 007	-0 009	-0 011	-0 014	-0 016	-0 019	-0 022	-0 024	-0 024	-0 016	-0 002
16	0 340	-0 007	-0 007	-0 008	-0 010	-0 012	-0 015	-0 018	-0 021	-0 023	-0 025	-0 023	-0 010	0 005
17	0 370	-0 007	-0 008	-0 009	-0 011	-0 014	-0 016	-0 019	-0 022	-0 025	-0 026	-0 019	0 001	0 014
18	0 400	-0 008	-0 009	-0 010	-0 013	-0 015	-0 019	-0 021	-0 024	-0 026	-0 024	-0 009	0 016	0 021
19	0 430	-0 009	-0 010	-0 012	-0 015	-0 018	-0 021	-0 024	-0 025	-0 025	-0 017	0 008	0 030	0 023
20	0 460	-0 011	-0 012	-0 015	-0 018	-0 021	-0 023	-0 025	-0 025	-0 020	-0 002	0 031	0 039	0 022
21	0 490	-0 013	-0 015	-0 018	-0 021	-0 023	-0 024	-0 024	-0 020	-0 008	0 022	0 050	0 038	0 019
22	0 520	-0 016	-0 018	-0 021	-0 023	-0 024	-0 022	-0 018	-0 008	0 015	0 051	0 055	0 031	0 016
23	0 550	-0 018	-0 021	-0 022	-0 022	-0 020	-0 014	-0 004	0 015	0 047	0 069	0 044	0 024	0 013
24	0 580	-0 020	-0 020	-0 019	-0 015	-0 008	0 003	0 021	0 048	0 074	0 059	0 032	0 019	0 011
25	0 610	-0 017	-0 014	-0 009	0 001	0 014	0 032	0 055	0 075	0 068	0 040	0 025	0 016	0 010
26	0 640	-0 005	0 003	0 014	0 029	0 047	0 064	0 075	0 069	0 046	0 030	0 021	0 015	0 009
27	0 670	0 017	0 031	0 046	0 059	0 068	0 070	0 063	0 046	0 034	0 025	0 019	0 013	0 008
28	0 700	0 040	0 053	0 060	0 063	0 060	0 053	0 044	0 036	0 029	0 022	0 017	0 012	0 008
29	0 730	0 052	0 054	0 052	0 049	0 045	0 041	0 036	0 030	0 025	0 020	0 016	0 012	0 007
30	0 760	0 048	0 045	0 042	0 040	0 037	0 034	0 031	0 027	0 022	0 018	0 015	0 011	0 007
31	0 790	0 040	0 038	0 036	0 035	0 032	0 030	0 027	0 024	0 021	0 017	0 014	0 010	0 007
32	0 820	0 034	0 033	0 032	0 031	0 029	0 027	0 025	0 022	0 019	0 016	0 013	0 010	0 007
33	0 850	0 029	0 029	0 028	0 027	0 026	0 024	0 022	0 020	0 018	0 015	0 012	0 010	0 006
34	0 879	0 025	0 025	0 025	0 024	0 023	0 022	0 020	0 018	0 016	0 014	0 011	0 009	0 006
35	0 907	0 022	0 022	0 022	0 022	0 021	0 020	0 018	0 016	0 014	0 012	0 010	0 008	0 005
36	0 933	0 019	0 020	0 020	0 019	0 019	0 018	0 016	0 015	0 013	0 011	0 009	0 007	0 005
37	0 957	0 017	0 018	0 018	0 018	0 017	0 016	0 015	0 014	0 012	0 010	0 008	0 007	0 005
38	0 979	0 015	0 016	0 016	0 015	0 015	0 014	0 013	0 012	0 011	0 009	0 007	0 006	0 004
39	1 000	0 011	0 013	0 013	0 013	0 012	0 012	0 011	0 010	0 009	0 007	0 006	0 005	0 004

CYCLE =

## FOURIER COEFFICIENTS FOR UPPER SURFACE PRESSURES A2 TERM

SPAN STATIONS/ETA

INDEX XI -0 10 0 2/ 0 3/ 0 4/ 0 5/ 0 6/ 0 7/ 0 8/ 0 9/ 0 19 0 29 0 39 0 49 0 58 0 68 0 77 0 84 0 90 0 95

## FOURIER COEFFICIENTS FOR UPPER SURFACE PRESSURES B1 TERM

CYCLE = 3

INDEX	XI	SPAN STATIONS/ETA												
		1/ -0 10	2/ 0 00	3/ 0 10	4/ 0 19	5/ 0 29	6/ 0 39	7/ 0 49	8/ 0 58	9/ 0 68	10/ 0 77	11/ 0 84	12/ 0 90	13/ 0 95
1	0 005	0 041	0 037	0 047	0 054	0 059	0 063	0 066	0 070	0 073	0 077	0 080	0 082	0 079
2	0 015	0 066	0 033	0 041	0 047	0 051	0 055	0 059	0 063	0 067	0 071	0 074	0 077	0 073
3	0 025	0 072	0 030	0 035	0 041	0 045	0 049	0 053	0 056	0 061	0 065	0 069	0 072	0 067
4	0 037	0 058	0 027	0 032	0 036	0 040	0 044	0 047	0 051	0 055	0 060	0 064	0 067	0 061
5	0 049	0 044	0 025	0 029	0 033	0 036	0 040	0 043	0 047	0 051	0 055	0 059	0 062	0 055
6	0 065	0 035	0 023	0 027	0 030	0 033	0 036	0 040	0 043	0 047	0 051	0 055	0 059	0 050
7	0 084	0 030	0 022	0 025	0 028	0 031	0 034	0 037	0 040	0 044	0 048	0 052	0 056	0 043
8	0 107	0 027	0 021	0 023	0 026	0 029	0 031	0 034	0 038	0 042	0 046	0 051	0 051	0 037
9	0 132	0 024	0 021	0 022	0 025	0 027	0 030	0 033	0 036	0 040	0 045	0 048	0 046	0 034
10	0 161	0 023	0 020	0 021	0 023	0 026	0 028	0 031	0 035	0 038	0 042	0 044	0 043	0 032
11	0 190	0 022	0 020	0 021	0 022	0 024	0 027	0 030	0 033	0 037	0 040	0 043	0 042	0 032
12	0 220	0 021	0 019	0 020	0 022	0 024	0 026	0 029	0 032	0 035	0 039	0 042	0 042	0 032
13	0 250	0 020	0 019	0 020	0 021	0 023	0 025	0 028	0 031	0 035	0 039	0 043	0 044	0 034
14	0 280	0 020	0 019	0 019	0 021	0 022	0 024	0 027	0 031	0 035	0 040	0 046	0 047	0 036
15	0 310	0 020	0 019	0 019	0 020	0 022	0 024	0 028	0 032	0 037	0 043	0 050	0 052	0 038
16	0 340	0 019	0 019	0 019	0 020	0 022	0 025	0 029	0 033	0 039	0 047	0 057	0 057	0 037
17	0 370	0 019	0 019	0 019	0 021	0 023	0 026	0 030	0 036	0 044	0 055	0 066	0 060	0 032
18	0 400	0 019	0 019	0 020	0 021	0 024	0 028	0 034	0 041	0 051	0 066	0 076	0 057	0 023
19	0 430	0 019	0 020	0 021	0 023	0 027	0 032	0 039	0 048	0 062	0 080	0 081	0 044	0 012
20	0 460	0 020	0 021	0 023	0 026	0 032	0 038	0 047	0 060	0 077	0 092	0 073	0 025	0 004
21	0 490	0 022	0 024	0 027	0 032	0 039	0 048	0 059	0 074	0 092	0 096	0 049	0 006	-0 001
22	0 520	0 025	0 029	0 034	0 041	0 050	0 061	0 075	0 091	0 103	0 080	0 015	-0 005	-0 003
23	0 550	0 032	0 037	0 045	0 054	0 065	0 078	0 091	0 104	0 103	0 062	-0 005	-0 013	-0 006
24	0 580	0 042	0 050	0 060	0 071	0 082	0 094	0 104	0 103	0 062	-0 005	-0 013	-0 006	-0 002
25	0 610	0 056	0 066	0 077	0 088	0 097	0 103	0 098	0 066	0 005	-0 020	-0 010	-0 003	-0 001
26	0 640	0 072	0 082	0 091	0 096	0 094	0 082	0 052	0 006	-0 022	-0 014	-0 006	-0 002	0 000
27	0 670	0 080	0 085	0 082	0 072	0 053	0 028	-0 001	-0 020	-0 015	-0 008	-0 003	-0 001	0 000
28	0 700	0 066	0 056	0 042	0 025	0 008	-0 007	-0 013	-0 012	-0 008	-0 004	-0 002	0 000	0 000
29	0 730	0 037	0 022	0 010	0 003	-0 002	-0 005	-0 007	-0 006	-0 005	-0 003	-0 001	0 000	0 000
30	0 760	0 014	0 008	0 005	0 002	0 000	-0 002	-0 003	-0 004	-0 003	-0 002	-0 001	0 000	0 001
31	0 790	0 005	0 005	0 003	0 002	0 000	-0 001	-0 002	-0 002	-0 002	-0 001	0 000	0 000	0 001
32	0 820	0 003	0 003	0 002	0 001	0 000	0 000	-0 001	-0 001	-0 001	-0 001	0 000	0 000	0 001
33	0 850	0 002	0 002	0 002	0 001	0 000	0 000	-0 001	-0 001	-0 001	-0 001	0 000	0 000	0 000
34	0 879	0 001	0 001	0 001	0 001	0 000	0 000	0 000	-0 001	-0 001	-0 001	-0 001	0 000	0 000
35	0 907	0 001	0 001	0 001	0 001	0 000	0 000	0 000	0 000	0 000	0 000	-0 001	0 000	0 000
36	0 933	0 001	0 001	0 001	0 001	0 001	0 000	0 000	0 000	0 000	0 000	-0 001	-0 001	-0 001
37	0 957	0 001	0 001	0 001	0 001	0 001	0 000	0 000	0 000	0 000	0 000	-0 001	-0 002	-0 003
38	0 979	0 001	0 001	0 001	0 001	0 001	0 001	0 000	0 000	0 000	0 000	-0 001	-0 002	-0 005
39	1 000	0 001	0 001	0 001	0 001	0 001	0 001	0 001	0 001	0 001	0 000	-0 001	-0 003	-0 009

## FOURIER COEFFICIENTS FOR UPPER SURFACE PRESSURES B2 TERM

CYCLE = 3

INDEX	XI	SPAN STATIONS/ETA												
		1/ -0 10	2/ 0 00	3/ 0 10	4/ 0 19	5/ 0 29	6/ 0 39	7/ 0 49	8/ 0 58	9/ 0 68	10/ 0 77	11/ 0 84	12/ 0 90	13/ 0 95
1	0 005	0 000	0 000	0 000	0 001	0 001	0 001	0 001	0 001	0 002	0 002	0 001	0 001	0 000
2	0 015	0 000	0 000	0 000	0 001	0 001	0 001	0 001	0 001	0 001	0 001	0 001	0 001	0 000
3	0 025	0 000	0 000	0 000	0 000	0 001	0 001	0 001	0 001	0 001	0 001	0 001	0 000	0 000
4	0 037	0 000	0 000	0 000	0 000	0 000	0 001	0 001	0 001	0 001	0 001	0 000	0 000	-0 001
5	0 049	0 000	0 000	0 000	0 000	0 000	0 000	0 001	0 001	0 001	0 000	0 000	0 000	-0 001
6	0 065	0 000	0 000	0 000	0 000	0 000	0 000	0 000	0 000	0 000	0 000	0 000	-0 001	-0 002
7	0 084	0 000	0 000	0 000	0 000	0 000	0 000	0 000	0 000	0 000	0 000	0 000	-0 001	-0 003
8	0 107	0 000	0 000	0 000	0 000	0 000	0 000	0 000	0 000	0 000	0 000	-0 001	-0 003	-0 003
9	0 132	0 000	0 000	0 000	0 001	0 001	0 001	0 001	0 000	0 000	-0 001	-0 002	-0 004	-0 003
10	0 161	0 000	0 000	0 001	0 001	0 001	0 001	0 001	0 000	-0 001	-0 002	-0 003	-0 003	-0 003
11	0 190	0 000	0 000	0 001	0 001	0 001	0 001	0 000	0 000	-0 001	-0 003	-0 004	-0 004	-0 003
12	0 220	0 000	0 001	0 001	0 001	0 001	0 000	0 000	-0 001	-0 002	-0 003	-0 005	-0 005	-0 002
13	0 250	0 001	0 001	0 001	0 001	0 001	0 000	0 000	-0 001	-0 003	-0 005	-0 006	-0 005	0 000
14	0 280	0 001	0 001	0 001	0 001	0 000	0 000	-0 001	-0 002	-0 004	-0 007	-0 008	-0 005	0 002
15	0 310	0 001	0 001	0 001	0 001	0 000	0 000	-0 002	-0 004	-0 006	-0 009	-0 008	-0 002	0 007
16	0 340	0 001	0 001	0 001	0 000	0 000	-0 001	-0 003	-0 006	-0 009	-0 011	-0 007	0 004	0 011
17	0 370	0 001	0 001	0 000	0 000	-0 001	-0 003	-0 005	-0 009	-0 012	-0 012	-0 002	0 012	0 013
18	0 400	0 001	0 000	0 000	-0 001	-0 002	-0 005	-0 009	-0 013	-0 014	-0 009	0 009	0 019	0 011
19	0 430	0 000	0 000	-0 001	-0 003	-0 005	-0 009	-0 013	-0 016	-0 013	0 002	0 022	0 019	0 007
20	0 460	-0 001	-0 001	-0 003	-0 006	-0 010	-0 014	-0 016	-0 015	-0 004	0 019	0 028	0 011	0 003
21	0 490	-0 002	-0 004	-0 007	-0 010	-0 014	-0 017	-0 015	-0 006	0 014	0 034	0 019	0 003	0 000
22	0 520	-0 005	-0 007	-0 011	-0 015	-0 016	-0 014	-0 005	0 012	0 034	0 031	0 004	-0 001	-0 001
23	0 550	-0 008	-0 011	-0 014	-0 014	-0 011	-0 001	0 014	0 033	0 037	0 008	-0 003	-0 002	-0 001
24	0 580	-0 010	-0 012	-0 010	-0 005	0 006	0 020	0 034	0 037	0 012	-0 006	-0 003	-0 002	-0 001
25	0 610	-0 007	-0 004	0 004	0 014	0 025	0 033	0 030	0 009	-0 008	-0 005	-0 003	-0 002	-0 001
26	0 640	0 003	0 011	0 020	0 025	0 024	0 016	0 001	-0 009	-0 006	-0 004	-0 002	-0 002	-0 001
27	0 670	0 010	0 015	0 014	0 009	0 001	-0 006	-0 010	-0 005	-0 003	-0 003	-0 002	-0 001	-0 001
28	0 700	0 009	0 003	-0 002	-0 006	-0 007	-0 005	-0 003	-0 003	-0 003	-0 002	-0 002	-0 001	-0 001
29	0 730	0 002	-0 003	-0 004	-0 003	-0 002	-0 002	-0 002	-0 002	-0 002	-0 002	-0 001	-0 001	-0 001
30	0 760	-0 002	-0 001	-0 001	-0 001	-0 001	-0 001	-0 001	-0 001	-0 001	-0 001	-0 001	-0 001	0 000
31	0 790	0 000	0 000	0 000	0 000	0 000	-0 001	-0 001	-0 001	-0 001	-0 001	-0 001	-0 001	0 000
32	0 820	0 000	0 000	0 000	0 000	0 000	0 000	-0 001	-0 001	-0 001	-0 001	-0 001	-0 001	0 000
33	0 850	0 000	0 000	0 000	0 000	0 000	0 000	-0 001	-0 001	-0 001	-0 001	-0 001	0 000	0 000
34	0 879	0 000	0 000	0 000	0 000	0 000	0 000	0 000	-0 001	-0 001	-0 001	0 000	0 000	0 000
35	0 907	0 000	0 000	0 000	0 000	0 000	0 000	0 000	0 000	0 000	0 000	0 000	0 000	0 000
36	0 933	0 000	0 000	0 000	0 000	0 000	0 000	0 000	0 000	0 000	0 000	0 000	0 000	0 000
37	0 957	0 000	0 000	0 000	0 000	0 000	0 000	0 000	0 000	0 000	0 000	0 000	0 000	0 000
38	0 979	0 000	0 000	0 000	0 000	0 000	0 000	0 000	0 000	0 000	0 000	0 000	0 000	0 000
39	1 000	0 000	0 000	0 000	0 000	0 000	0 000	0 000	0 000	0 000	0 000	0 000	0 000	0 000

\*\*\*\*\*  
\*\*\* Note ATRAN3S prints similar output for lower surface pressures \*\*\*  
\*\*\* and pressure differences. The corresponding results for \*\*\*  
\*\*\* magnitudes and phase angles are also computed and printed \*\*\*  
\*\*\*\*\*

MAGNITUDES AND PHASE ANGLES FOR LIFT AND MOMENT COEFFICIENTS

CYCLE = 3

INDEX	XI	SPAN STATIONS/ETA											
		1/ -0 10	2/ 0 00	3/ 0 10	4/ 0 19	5/ 0 29	6/ 0 39	7/ 0 49	8/ 0 58	9/ 0 68	10/ 0 77	11/ 0 84	12/ 0 90

MAGNITUDE OF LIFT COEFFICIENTS

0 00000 0 05040 0 04924 0 04786 0 04597 0 04353 0 04050 0 03679 0 03237 0 02732 0 02187 0 01616 0 00971

PHASE ANGLE OF LIFT COEFFICIENTS

0 00 170 08 169 99 170 45 171 07 171 76 172 45 173 10 173 64 173 99 174 02 173 44 171 22

MAGNITUDE OF MOMENT COEFFICIENTS

0 00000 0 00963 0 00908 0 00850 0 00782 0 00706 0 00624 0 00538 0 00449 0 00361 0 00278 0 00200 0.00116

PHASE ANGLE OF MOMENT COEFFICIENTS

0 00 254 57 250 25 245 86 241 59 237 26 232 70 227 79 222 53 217 24 212 34 208 16 204 54

## REFERENCES

1. Goorjian, P. M.: Computations of Unsteady transonic Flows. Advances in Computational Transonics. Vol. IV, Recent Advances in Numerical Methods in Fluid, W. G. Habashi, ed., Pineridge Press Ltd. (U.K.), Mar. 1984.
2. Ballhaus, W. F.; Deiwert, G. S.; Goorjian, P. M.; Holst, T. L.; and Kutler, P.: Advances and Opportunities in Transonic Flow Computations. Numerical and Physical Aspects of Aerodynamic Flows, Springer, 1981.
3. Ashley, H.: Role of Shocks in the "Sub-Transonic" Flutter Phenomenon. *J. Aircraft*, vol. 17, Mar. 1980, pp. 187-197.
4. Ballhaus, W. F.; and Goorjian, P. M.: Implicit Finite Difference Computations of Unsteady Transonic Flows about Airfoils. *AIAA J.*, vol. 15, Dec. 1977, pp. 1728-1735.
5. Traci, R. M.; Albano, E. D.; and Farr, J. L.: Small Disturbance Transonic Flows about Oscillating Airfoils and Planar Wings. TR-75-100, Air Force Flight Dynamics Laboratory, Dayton, OH, June 1975.
6. Eastep, F. E.; and Olsen, J. J.: Transonic Flutter Analysis of a Rectangular Wing with Conventional Airfoil Sections. *AIAA J.*, vol. 18, no. 10, Oct. 1980, pp. 1159-1164.
7. Borland, C. J.; and Rizzetta, D. P.: Transonic Unsteady Aerodynamics for Aeroelastic Applications. Vol. I. Technical Development Summary for XTRAN3S. TR-80-3107, Air Force Wright Aeronautical Laboratory, Dayton, OH, June 1982.
8. Guruswamy, P.; and Goorjian, P. M.: Comparison between Computational and Experimental Data in Unsteady Three Dimensional Transonic Aerodynamics Including Aeroelastic Applications. AIAA Paper 82-0690-CP, 1982.
9. Myers, M. R.; Guruswamy, P.; and Goorjian, P. M.: Flutter Analysis of a Transport Wing Using XTRAN3S. AIAA Paper 83-0922, 1983.
10. Seidel, D. A.; Bennett, R. M.; and Ricketts, R. H.: Some Recent Applications of XTRAN3S. NASA TM-85641, 1983.
11. Yoshihara, H.: Formulation of the Three-Dimensional Transonic Unsteady Aerodynamic Problem. TR-79-3030, Air Force Flight Dynamics Laboratory, Dayton, OH, Feb. 1979.
12. Lomax, H.; Bailey, F. R.; and Ballhaus, W. F.: On the Numerical Simulation of Three-Dimensional Transonic Flow with Application to the C-141 Wing. NASA TN D-6933, 1973.

13. Ballhaus, W. F.; and Bailey, F. R.: Numerical Calculation of Transonic Flow about Swept Wings. AIAA Paper 72-677, 1972.
14. Guruswamy, P.; and Goorjian, P. M.: An Efficient Coordinate Transformation Technique for Unsteady Transonic Aerodynamic Analysis of Low Aspect Ratio Wings. AIAA Paper 84-0872-CP, Palm Springs, Calif., May 1984.
15. Jameson, A.: Iterative Solution of Transonic Flows over Airfoils and Wings, Including Flows at Mach 1. *Commun. Pure Appl. Math.*, vol. 27, 1974, pp. 283-309.
16. Rizzetta, D. P.; and Borland, C. J.: Numerical Solution of Three-Dimensional Unsteady Transonic Flow over Wings Including Inviscid/Viscous Interactions. NASA CR-166561, 1984.
17. Marstiller, J. W.; Guruswamy, P.; Yang, T. Y.; and Goorjian, P. M.: Effects of Viscosity and Modes on Transonic Flutter Boundaries of Wings. AIAA Paper 84-0870-CP, Palm Springs, Calif., 1984.
18. Guruswamy, P.; and Goorjian, P. M.: Transonic Aeroelastic Analysis of the B-1 Wing. AIAA Paper 85-0690-CP, Orlando, Fla., 1985.
19. Ballhaus, W. F.; and Goorjian, P. M.: Computation of Unsteady Transonic Flows by the Indicial Method. *AIAA J.*, vol. 16, no. 2, Feb. 1978, pp. 117-124.
20. Guruswamy, P.; and Yang, T. Y.: Aeroelastic Time Response Analysis of Thin Airfoils by Transonic Code LTRAN2. *Computers and Fluids*, vol. 9, no. 4, Dec. 1980, pp. 409-425.
21. Tijdeman, J. et al.: Transonic Wind Tunnel Tests on an Oscillating Wing with External Stores. Pt. II. The Clean Wing. TR-78-194, Air Force Flight Dynamics Laboratory, Dayton, OH, Mar. 1979.

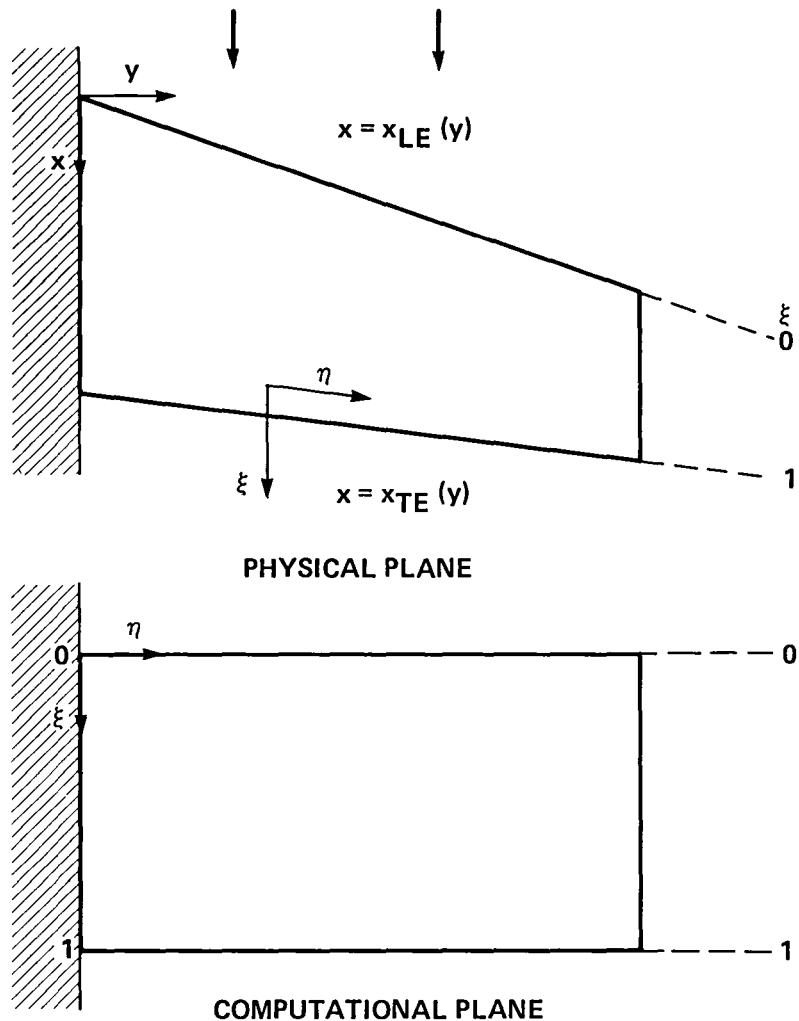


Figure 1.- Wing planform transformation.

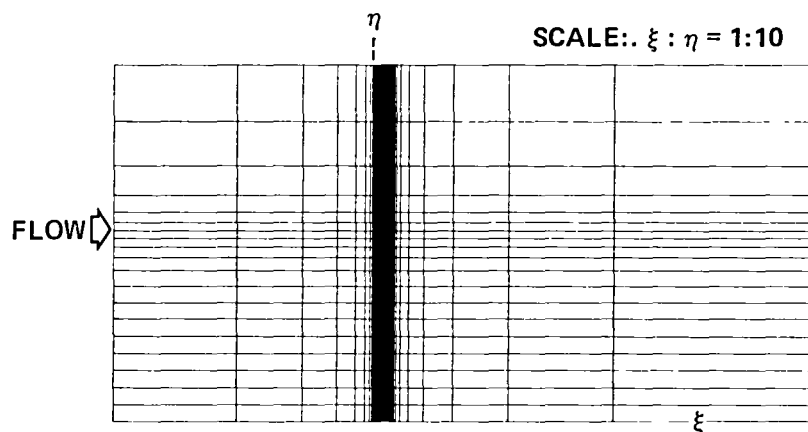


Figure 2.- Computational mesh (64  $\times$  20):  $\xi$ - $\eta$  plane.

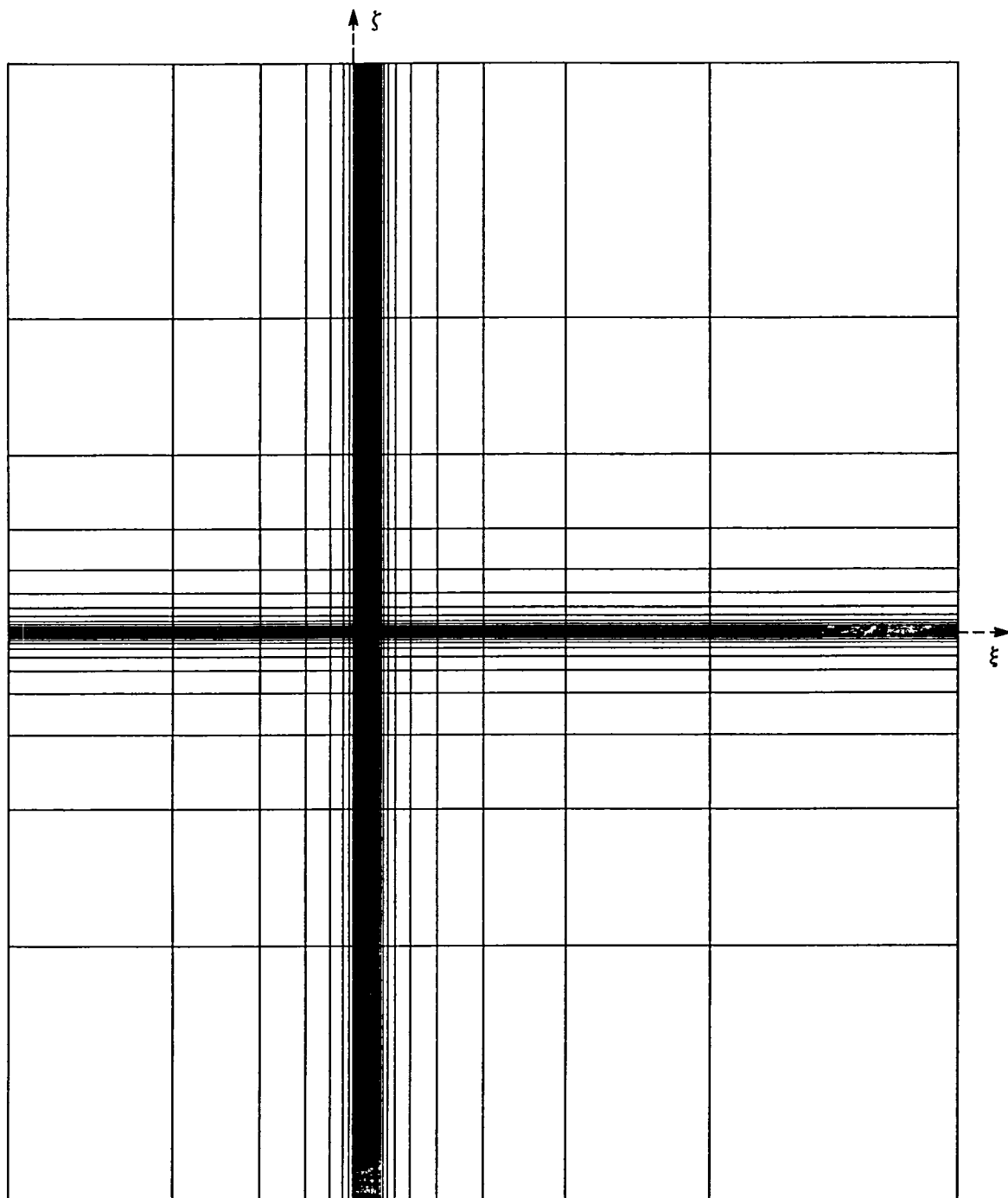


Figure 3.- Computational mesh (64  $\times$  40):  $\xi$ - $\eta$  plane.

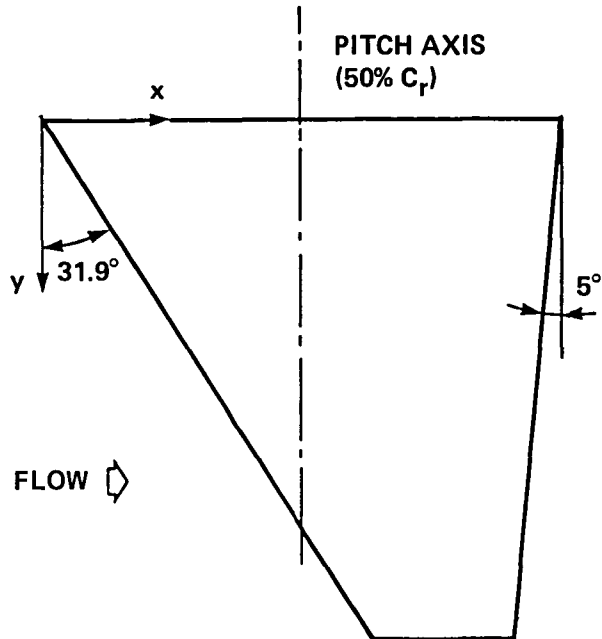


Figure 4.- Planform of the F-5 wing: aspect ratio = 2.98, taper ratio = 0.31, leading-edge sweep =  $32^\circ$ .

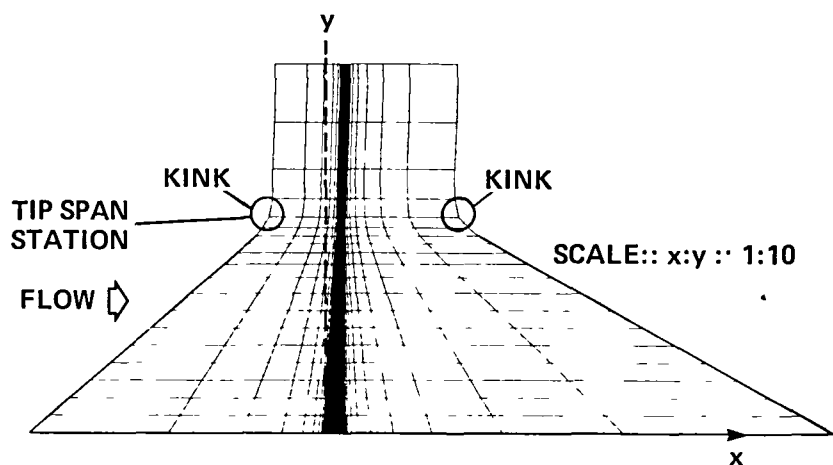


Figure 5.- Physical mesh ( $64 \times 20$ ) in  $x$ - $y$  plane: conventional shearing transformation.

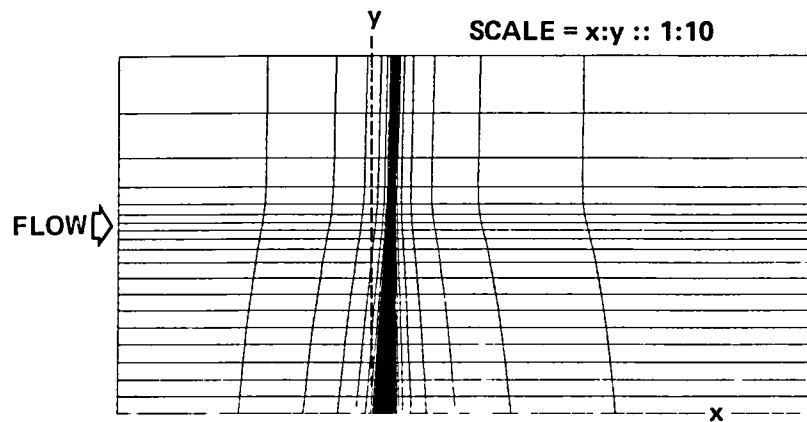


Figure 6.- Physical mesh (64 v 20) in x-y plane: modified shearing transformation.

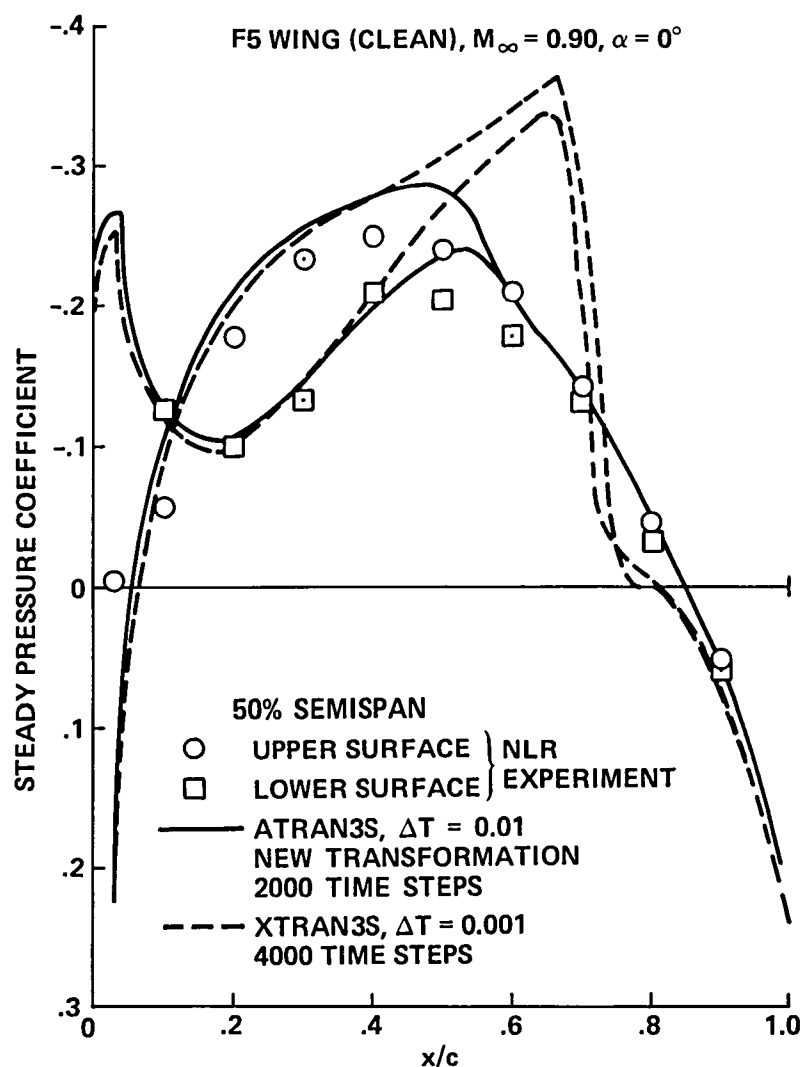


Figure 7.- Effect of transformation on steady pressures: clean F-5 wing,  $M_{\infty} = 0.90, \alpha = 0^\circ$ .

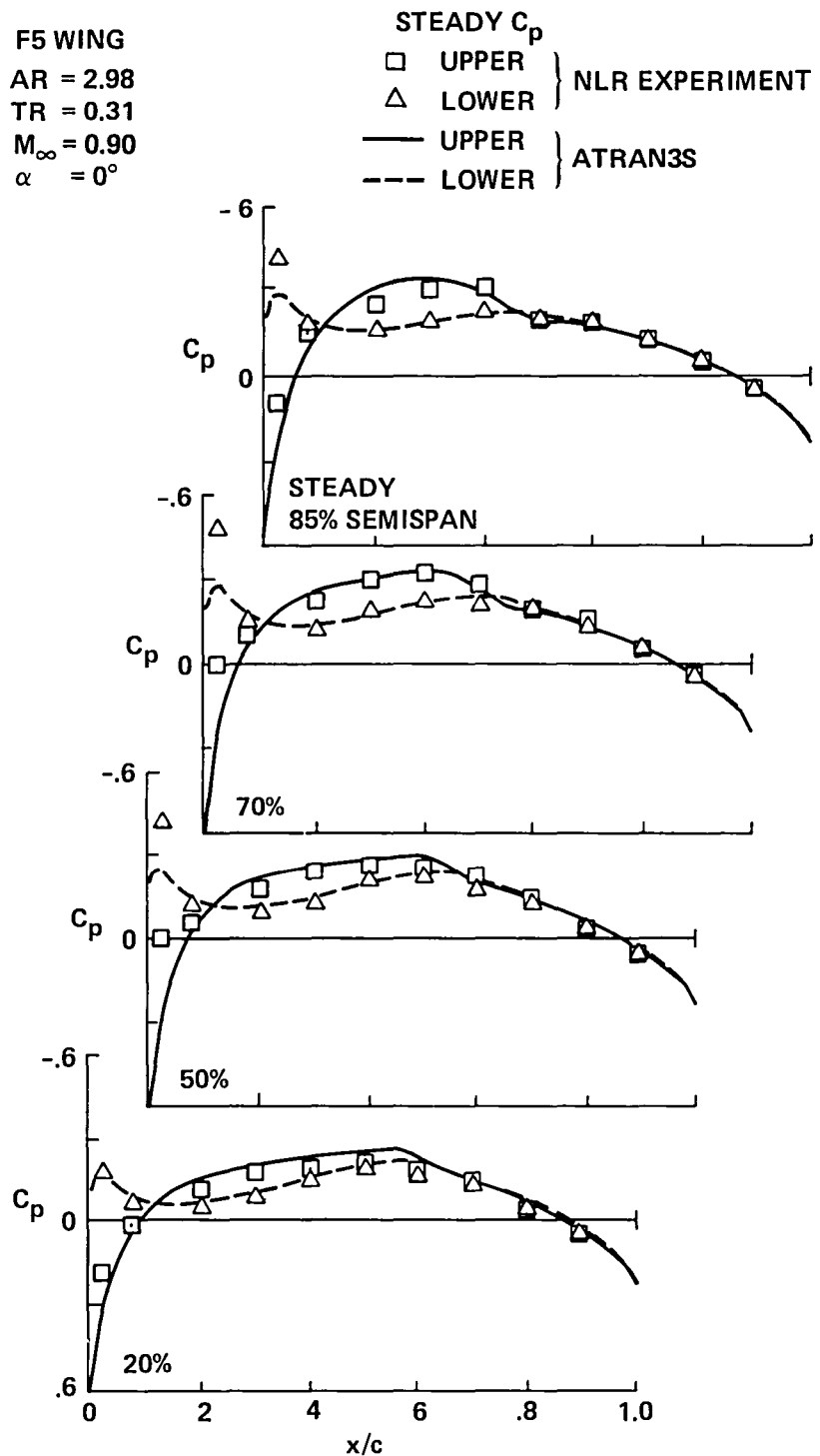


Figure 8.- Comparison of steady pressures between theory and experiment for F-5 wing: aspect ratio = 2.98, taper ratio = 0.31,  $M_{\infty} = 0.90$ ,  $\alpha = 0^\circ$ .

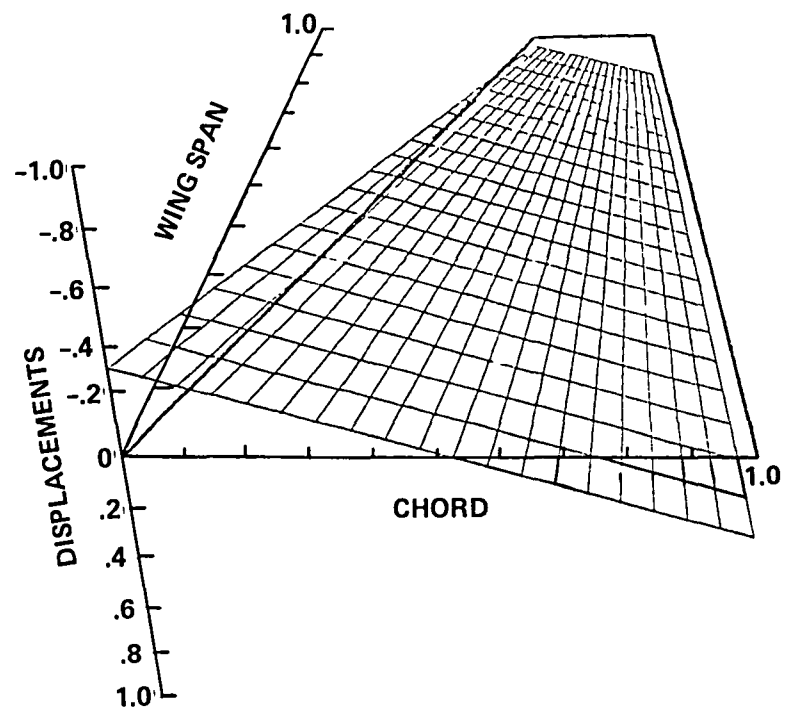


Figure 9.- Unsteady modal motion of the F-5 wing.

F5 WING  
 AR = 2.98  
 TR = 0.31  
 $M_\infty = 0.90$   
 $\alpha = 0^\circ$   
 $t = 40$  Hz

UNSTEADY UPPER SURFACE  $C_p$   
 — REAL  
 - - - IMAGINARY } ATRAN3S  
 □ REAL  
 △ IMAGINARY } NLR EXPERIMENT

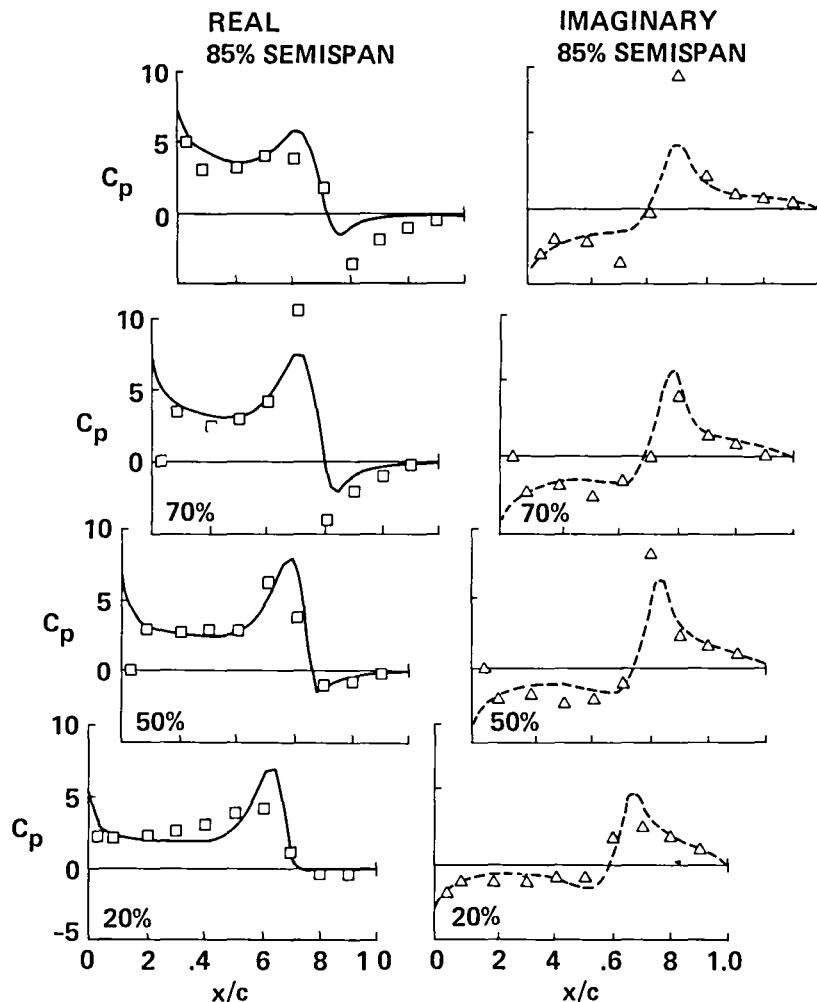


Figure 10.- Comparison of unsteady upper-surface pressures on F-5 wing from theory and experiment: aspect ratio = 2.98, taper ratio = 0.31,  $M_\infty = 0.90$ ,  $\alpha = 0^\circ$ ,  $t = 40$  Hz.

1 Report No NASA TM-86783	2 Government Accession No	3 Recipient's Catalog No	
4 Title and Subtitle  ATRAN3S: AN UNSTEADY TRANSONIC CODE FOR CLEAN WINGS		5 Report Date December 1985	
7 Author(s) Guru P. Guruswamy,* Peter M. Goorjian, and Fergus J. Merritt*		6 Performing Organization Code	
9 Performing Organization Name and Address Ames Research Center, Moffett Field, CA 94035  *Informatics General Corp. Palo Alto, CA 94303.		8 Performing Organization Report No A-85359	
12 Sponsoring Agency Name and Address National Aeronautics and Space Administration Washington, DC 20546		10 Work Unit No	
		11 Contract or Grant No	
		13 Type of Report and Period Covered Technical Memorandum	
		14 Sponsoring Agency Code 505-60-0	
15 Supplementary Notes  Point of contact: Guru P. Guruswamy, Ames Research Center, MS 202A-14, Moffett Field, CA 94035 (415)694-6329 or FTS 464-6329			
16 Abstract  This report explains the development and applications of the unsteady transonic code ATRAN3S for clean wings. Explanations of the unsteady, transonic small-disturbance aerodynamic equations that are used and their solution procedures are discussed. A detailed user's guide, along with input and output for a sample case, is given.			
17 Key Words (Suggested by Author(s)) Computational aerodynamics Transonics Aeroelasticity Clean wings Unsteady		18 Distribution Statement Unlimited	
Subject category - 02			
19 Security Classif (of this report) Unclassified	20 Security Classif (of this page) Unclassified	21 No of Pages 51	22 Price* A03

**End of Document**